GDR NANOMATERIALS FOR ENERGY APPLICATIONS

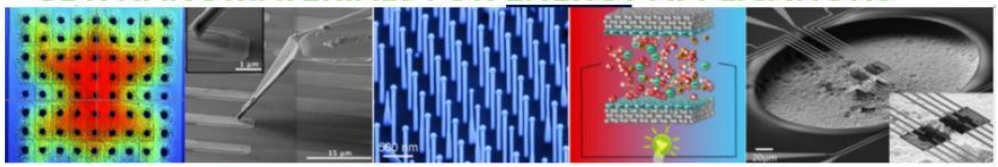

RENNES, Campus de Beaulieu 08 – 10 novembre 2023

Pôle Numérique Rennes Beaulieu (PNRB, Bâtiment 9B)

SPONSORS

RENATECH
Le réseau français de nanofabrication

ribori
INSTRUMENTATION

SCAN MAT
SCAN MAT

NANO-PHOT
Nano-Optics & Nanophotonics Graduate School
utt
cnrs
Université de Reims Champagne-Ardenne

INSTITUT foton

CSM
Institut des Sciences Chimiques de Rennes
UMR CNRS 6226

lumomat

Liste des participants

- Amara Mohamed
- Anthony Szymczyk
- Arnault Jean-Charles
- Artero Vincent
- Aurélien Roux
- Bahout Mona
- Belrhiti Nejjar Rachid
- Ben-Abdallah Philippe
- Bergonzoni Ashanti
- Bertru Nicolas
- Bescond Marc
- Bourgeois Olivier
- Brisuda Boris
- Combe Nicolas
- Cordier Stéphane
- Cornet Charles
- Costuas Karine
- Dursap Thomas
- El Fatimy Anass
- El Hajj Julien
- El Kari Hamza
- Ezzahri Younes
- Fihey Arnaud
- Gautheron-Bernard Rozenn
- Gautier Regis

- Ghanem Mohamad
- Girard Hugues
- Gómez Viloria Mauricio
- Grasset Fabien
- Guilloux-Viry Maryline
- Herlin-Boime Nathalie
- Herz Florian
- Isaiev Mykola
- Jiang Junke
- Khater Antoine
- Kyrychenko Nataliia
- Lagrost Corinne
- Le Hanh Vi
- Léger Yoan
- Loison Owen
- Maire Jérémie
- Merabia Samy
- Messina Riccardo
- Nakamae Sawako
- Nataf Guillaume
- Nkenfack Isibert
- Paofai Serge
- Paulatto Lorenzo
- Poirot Nathalie
- Poulos Markos
- Renaud Adèle
- Robillard Jean-Francois
- Romanin Davide
- Sáenz De Santa María Modroño Pablo
- Saint-Martin Jérôme
- Santos Almeida Joseane
- Sjakste Jelena

- Surble Suzy
- Teffo Céline
- Termentzidis Konstantinos
- Tessier Franck
- Thébaud Simon
- Tyrpenou Christos
- Verger Louisiane
- Volonakis George
- Xu Ze-Li
- Zhang Xiao

Résumés des présentations

CONFÉRENCIERS INVITÉS

● Corinne Chanéac - Mercredi 08 novembre, 14h00

Strength and Weakness of Temperature Measurment Using Luminescent Nanoparticles

corinne.chaneac@sorbonne-universite.fr

Laboratoire de Chimie de la Matière Condensée de Paris

Corinne Chanéac is Professor at Sorbonne Université since 2009 in the Chemistry Department. She's working in Laboratoire Chimie de la Matière Condensée de Paris (LCMCP, UMR 7574 CNRS-Sorbonne Univ., Paris) that is French pioneer lab in the field of sol-gel processes. She works on the design of nanoparticles with tunable properties through bottom-up approach by mean of soft and green chemistry. Her research activity is focused on the synthesis of original oxide nanomaterials (metallic, doped and hybrid organic-inorganic), with broader chemical composition, crystalline structure, size and shape. She develops innovative nanoparticles synthesis based on microwave assisted nucleation and growth process. She studies the influence of the chemical conditions of precipitation on the first stages of nucleation and growth of nanoparticles and the impact of surface energies on the thermodynamic stabilization of metal oxide morphologies. She has gained a strong expertise in the field of luminescent nanoparticles for long lasting imaging and nanothermometry.

She is in charge of the coordination of the *Nano group in LCMCP* and is at the head of the National Center of Competences in *Nano Sciences (UAR CNRS 2205)*. She has published 140 peer-reviewed articles, 7 book chapters and produced 8 international patents

● Jacky Even - Jeudi 09 novembre, 9h00

Tuning the properties of 2D perovskites for photovoltaic applications

jacky.even@insa-rennes.fr

Fonctions Optiques pour les Technologies de l'information (Unité mixte 6082 CNRS) - Institut national des Sciences Appliquées (INSA) de Rennes

Jacky Even is full Professor at INSA Rennes engineering school and institute *FOTON* since 1999. He received a PhD in Physics from University Paris VI in 1992. He was associate professor at the Physics Department of Rennes University from 1992 to 1999, combining various experimental and theoretical approaches for phase transitions and chemical reactions in molecular solids. In 1999, he created FOTON

laboratory's simulation team focusing initially on III-V semiconductor nanostructures for optical telecommunications, and later on silicon photonics and photovoltaics. Starting in 2010, a joint simulation team was progressively built up between FOTON and *ISCR* CNRS labs in Rennes on the topic of emerging halide perovskite semiconductors. The group has strong collaborations for perovskite photovoltaics with the experimental groups of Aditya Mohite in Los Alamos National Lab., now Rice University, and Mercouri Kanatzidis in Northwestern University.

● Damien Voiry - Jeudi 09 novembre, 11h50

Nanochemistry on low-dimensional materials for electrocatalytic CO2 conversion and water depollution

damien.voiry@umontpellier.fr

Institut Européen des membranes

Damien Voiry received B. Eng degree in Materials Science from the Graduate School of Chemistry and Physics of Bordeaux, France in 2007. He obtained his PhD in Materials Science and Engineering from the Center Paul Pascal, University of Bordeaux in 2010 under the supervision of Dr. Alain Pénicaud. His PhD focused on the dissolution and covalent functionalization of carbon nanotubes. In 2011, he joined the group of Professor Chhowalla as postdoctoral associate to work on exfoliated 2D materials. Since February 2016, he is a CNRS researcher at the European Institute of Membranes (IEM, UMR5635) in Montpellier and was awarded an ERC-Starting grant and an ERC-Proof of Concept grant in 2018 and 2022. Damien Voiry has deposited 8 patents and published more than 65 research articles for a total number of citations greater than 18,500. He was received the CNRS Bronze Medal in 2020, the Young Researcher Award from the French Chemical Society (SCF) in 2022 and was nominated to the Young Academy of Europe in 2020. His research deals with the engineering of low dimensional materials for novel membranes and energy conversion

● Vincent Artero - Vendredi 10 novembre, 8h30

Bioinspired Catalysis and Hydrogen Technologies when Nanosciences and Electrocatalysis flow together

Laboratoire Chimie et Biologie des Métaux

vincent.artero@cea.fr

Vincent Artero (born 1973) is a graduate of the Ecole Normale Supérieure. He received a Ph.D. degree from UPMC (Univ. Paris 6) in 2000, working on polyoxometallates under the supervision of Prof. A. Proust. After a postdoctoral stay at RWTH Aachen with Prof. U. Kölle, he got a CEA scientist position in 2001 working with Prof. M. Fontecave in Grenoble. He's now Research Director at CEA and leads the Laboratoire de Chimie et Biologie des Métaux co-operated by Univ Grenoble Alpes, CNRS and CEA, where his group *SOLHYCAT* investigates bioinspired chemistry and artificial photosynthesis.

PRÉSENTATIONS ORALES

8-8 nov. 2023

Nanomaterials-Nanostructuration

Features of contact angle hysteresis at the nanoscale

Viktor Mandrolko[1], Sergii Burian[2], Guillaume Castanet[1], Yaroslav Grosu[3,4], Liudmila Klochko[5], David Lacroix[1], and Mykola Isaiev[1]

[1]*Université de Lorraine, CNRS, LEMTA, 54000 Nancy, France*
[2]*Faculty of Physics, Taras Shevchenko National University of Kyiv, 64 Volodymyrska Street, Kyiv 01601, Ukraine*
[3]*Centre for Cooperative Research on Alternative Energies (CIC energiGUNE), Basque Research and Technology Alliance (BRTA), Alava Technology Park, Albert Einstein 48, 01510 Vitoria-Gasteiz, Spain*
[4]*Institute of Chemistry, University of Silesia, Szkolna 9 street, 40-006 Katowice, Poland*
[5]*Université de Lorraine, CNRS, Inria, LORIA, 54000 Nancy, France*

Understanding the three-phase contact line between gas, liquid, and solid is important for numerous applications. Particularly, the line separating liquid/solid/vapor is important for thermal transport phenomena assisted with phase change. From this point of view, the movement of the three-phase contact line is crucial for describing heat dissipation/transformation efficiency. This movement may be considered because of external forces' action arising from the phase change process.

However, the three-phase contact line response on external force action at the nanoscale is still an open question. At the macroscale, such a response may be characterized by a contact angle hysteresis, and several models are presented in the literature for its description. However, there still needs to be more information concerning the hysteresis at the nanoscale.

During our talk, we will describe the application of the molecular dynamics approach for simulating a liquid droplet shape under an external force action for the different wetting regimes. Additionally, we will present the analytical model to evaluate the droplet shape. Fitting the results of the MD simulation with the analytical model allows us to evaluate the receding and advancing wetting angle of the nanoscale droplet. As the physical result, we stated the crucial role of the interplay between capillary forces and viscous forces on the droplet shape. We found that when capillary forces dominate, the contact angle hysteresis is well described by the macroscale Cox-Voinov model.

Generalized coupled dipole method for thermal far-field radiation

Florian HERZ[1,*] and Svend-Age Biehs[2]

[1] *Laboratoire Charles Fabry, UMR 8501, Institut d'Optique, CNRS, Université Paris-Saclay, 91127 Palaiseau Cedex, France*
[2] *Institut für Physik, Carl von Ossietzky Universität, D-26111 Oldenburg, Germany*

*florian.herz@institutoptique.fr

We introduce a many-body theory for thermal far-field emission of dipolar dielectric and metallic nanoparticles (NPs) close to a substrate within fluctuational electrodynamics. With this theory we can assign distinct temperatures to each NP, substrate, and background. We exemplary determine the radiation emitted by four separated NPs above a substrate composed of SiC and Ag. Moreover, we perform discrete dipole approximation (DDA) to model thermal emission of a SiO_2 particle in vacuum and thermal far-field radiation of a Si tip close to a SiC substrate. (F. Herz and S.-A. Biehs, *Phys. Rev. B* 105, 205422 (2022))

I. Introduction

The study of far-field emission in a heated system of point-like dipoles close to a substrate has become significantly more important during the last decade since the development of scattering near-field microscopes, e.g. SNoiM [1, 2] or TRSTM [3, 4]. To model such an experimental setup accurately, one has to consider the different temperatures of substrate, nanoparticles, and background, [5, 6] as well as eddy currents generated inside of the usually metallic microscope tip [7], which is approximated by the dipoles, probing the substrate.

II. Outline

Our model, that I would be happy to present, includes these key considerations so that it can be used to model heat transfer in systems of separated nanoparticles with different properties above a planar substrate (1b) or to perform discrete dipole approximation (DDA) of a macroscopic object (1a).

To investigate our model's robustness, I want to discuss the thermal radiation of a spherical SiO2 nanoparticle close to a SiO2 substrate and compare it with the radiation of same sphere approximated using DDA. Furthermore, I would like to show our results when applying it to model the thermal radiation of four particle assemblies of SiC and Ag nanoparticles above a planar SiC and Ag substrate. Finally, I want to present our calculation of the thermal far-field radiation of a sharp Si tip (1c) close to a SiC substrate using DDA and compare it with already existing results [8] (1d).

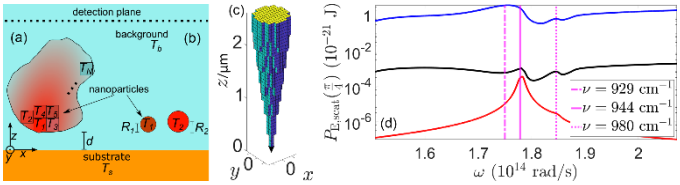

FIGURE 1. Scetch of the considered system (a-b), Model of a sharp tip (c), and Its DDA-results compared to single dipole models (d)

III. Conclusion

Our model generalizes previous models and is, therefore, very versatile. It can be used to study the thermal emission of dielectric and metallic particle assemblies close to a substrate within the coupled dipole method and to model thermal emission of a single or several macroscopic objects near a substrate within DDA. We are convinced that our generalized model will be very useful in further, more detailed studies of thermal emission of many-particle systems including substrates and the modelling of scattering-type experiments.

Acknowledgment

Florian Herz acknowledges financial support by the German Research Foundation under project number 519479175.

References

[1] K.-T. Lin, S. Komiyama, S. Kim, K. Kawamura, and Y. Kajihara, "A high signal-to-noise ratio passive near-field microscope equipped with a helium-free cryostat", *Rev. Sci. Instrum.*, vol. 88, p. 013706, 2017

[2] S. Komiyama, "Perspective: Nanoscopy of charge kinetics via terahertz fluctuation", *J. Appl. Phys.*, vol. 125, p. 010901, 2019

[3] A.C. Jones and M.B. Raschke, " Thermal Infrared Near-Field Spectroscopy", *Nano. Lett.*, vol. 12, p. 1475, 2012

[4] B.T. O'Callahan, W.E. Lewis, A.C. Jones, and M.B. Raschke, "Spectral frustration and spatial coherence in thermal near-field spectroscopy", *Phys. Rev. B*, vol. 89, p. 245446, 2014

[5] R. Messina, M. Tschikin, S.-A. Biehs, and P. Ben-Abdallah, "Fluctuation-electrodynamic theory and dynamics of heat transfer in systems of multiple dipoles", *Phys. rev. B*, vol. 88, p. 104407, 2013

[6] F. Herz and S.-A. Biehs, "Dipole model for far-field thermal emission of a nanoparticle above a planar substrate", *J. Quant. Spectrosc. Radiat. Transf.*, vol. 266, p. 107572, 2021

[7] J. Dong, J. Zhao, and L. Liu, "Radiative heat transfer in many-body systems: Coupled electric and magnetic dipole approach", *Phys. Rev. B*, vol. 95, p. 125411, 2017

[8] S. Edalatpour, V. Hatamipour, and M. Frankcoeur, "Spectral redshift of the thermal near field scattered by a probe", *Phys. Rev. B*, vol. 99, p. 165401, 2

Using the cluster route to nanostructure transition metal nitrides and carbides

F. Tessier[1], G. Dubois[1], T. Havet[1], , N. Dumait[1], S. Cordier[1], H. Kaper[2], F. Grasset[1], C. Tardivat[2], T. Uchikoshi[3,4], N. Ohashi[3,4]

[1] *Univ. Rennes, CNRS, Institut des Sciences Chimiques de Rennes, UMR 6226, 35000 Rennes, France*
[2] *CNRS-Saint-Gobain Research Provence, UMR 3080, Ceramic Synthesis and Functionalization Laboratory, 84306 Cavaillon, France*
[3] *CNRS-Saint-Gobain-NIMS, UMI 3629, Laboratory for Innovative Key Materials and Structures (LINK), National Institute for Materials Science, Tsukuba 305-0044, Japan*
[4] *Research Center for Functional Materials, National Institute for Materials Science, 305-0044 Tsukuba, Japan*

Transition metal nitrides (TMN) form a class of materials with unique physical and chemical properties. Among them, molybdenum nitrides are mainly used as high performance magnets or catalysts for a wide range of reactions [1]. This work aims at developing innovative syntheses to prepare nanostructured TMN from metallic clusters [2]. The use of a nanoscale precursor such as $(TBA)_2Mo_6Br_{14}$ (TBA= tetrabutylammonium) enables to reach different molybdenum nitride compositions (Mo_2N, Mo_5N_6) by thermal reaction under ammonia at relatively low temperatures. Such a novel synthetic approach highlights the prime importance of the starting material to stabilize specific stoichiometries [3-4] in comparison with the MoS_2 route. The same approach was developped between molybdenum-based clusters and sucrose or urea to form corresponding carbides, and then extended to other transition metals.

[1] J.S.J. Hargreaves, *Coord. Chem. Rev.* **2013**, 257, 2015.
[2] K. Kirakci, S. Cordier, C. Perrin, *Z. Anorg. Allg. Chem.* **2005**, 631, 411.
[3] R. Marchand, F. Tessier, F.J. DiSalvo, *J. Mater. Chem.* **1999**, 9, 297.
[4] K. Guy, F. Tessier, S. Cordier, H. Kaper, F. Grasset, N. Dumait, M. Nishio, Y. Matsushita, Y. Matsui, T. Takei, D. Lechevalier, C. Tardivat, T. Uchikoshi, N. Ohashi, *Chem. Mater.* **2020**, 32**,** 6026.

Phonon transport in asymmetric nanostructures in the ballistic regime

(Boris BRISUDA[1]), Jon CANOSA[2], Carlos A. POLANCO[3], Victor DOEBELE[1], Thierry CROZES[1], Jean.-François ROBILLARD[2], Natalio MINGO[3], Laurent SAMINDAYAR[1], Olivier BOURGEOIS[1]

[1]*Institut Néel, CNRS-Université Grenoble Alpes, 25 avenue des Martyrs, F-38000 Grenoble, France*
[2]*Univ. Lille, CNRS, Centrale Lille, Junia, Univ. Polytechnique Hauts-de-France, UMR 8520 – IEMN, F-59000 Lille, France*
[3]*CEA LITEN, 16 avenue des Martyrs, F-38000 Grenoble, France*

I. Introduction

The manipulation of heat fluxes is possible by acting on the transport of phonons at the nanoscale using advanced nanostructuration in what is currently called thermal metamaterials. This is one of the major challenges of the current small-scale energy management.

II. ABSTRACT

In our experiment we propose a suspended double-membrane based sensor, see Figure 1 top, functioning at very low temperatures (<100mK) using the state-of-the-art niobium nitride thermometry with attowatt sensitivity [1]. This will enable us to demonstrate innovative thermal effects involving large phonon mean-free-paths and long phonon-wavelength (>100nm) in the non-Fourier regime.

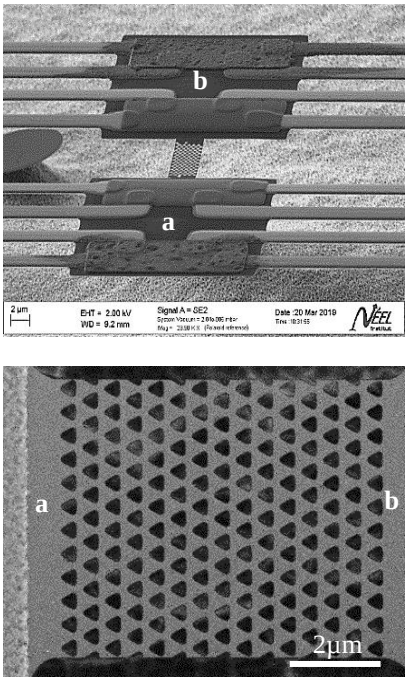

FIGURE 1. SEM IMAGES OF THE SUSPENDED MEMBRANES (TOP) AND THE NANOSTRUCTURED ASYMMETRIC SAMPLE (BOTTOM)

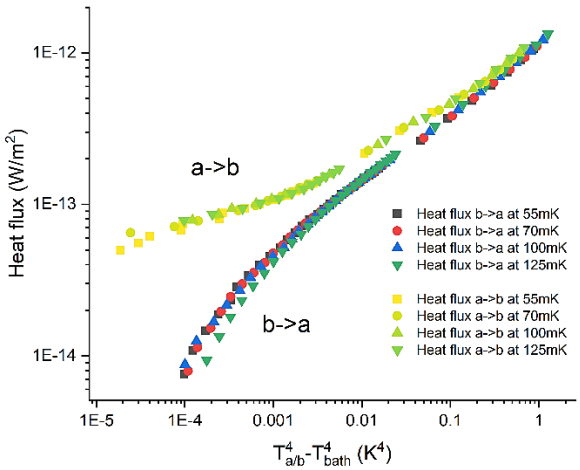

FIGURE 2. HEAT FLUX ON ONE MEMBRANE (a OR b) AS A FUNCTION OF THE DIFFERENCE BETWEEN $T^4_{membrane(a\,/\,b)}$ AND T^4_{bath}.

The sample (nanostructured layer of SiN), see Figure 1 bottom, is installed in between the membranes allowing the measurement of heat flux in both directions. They are nanostructured using microelectronic technology at the length scale of the phonon wavelength which is on the order of 100 nm at 1K in the case of silicon nitride. The length of the sample is inferior to the phonon mean-free path ensuring ballistic regime of phonon transport. Two types of nanostructured samples are studied in this study. One is a periodic system allowing the study of ballistic phononic transport in phononic crystal structures, the other is an anisotropic lattice meant for the study of thermal rectification.

This presentation will focus on the asymmetric sample shown in Figure 1. and the possible impact of the structure on the heat dissipation in the system [2]. In Figure 2, the heat fluxes are represented as a function of the temperature gradient applied between the two membranes (T_a T_b), and the heat bath T_{bath} showing potential asymmetry in phonon exchanges.

References

[1] A. Tavakoli, K. Lulla, T. Crozes, E. Collin, and O. Bourgeois, "Heat conduction in a ballistic 1D phonon waveguide indicate breakdown of the thermal conductance quantization", Nature Commun. 9, 4287 (2018).

[2] B. Brisuda, J. Canosa, C. Polanco, V. Doebele, T. Crozes, J.-F. Robillard, N. Mingo, L. Saminadayar, O. Bourgeois, article in preparation (2023).

Nanoscale Transport Properties

Phononic Energy Transport at Differential Material Nanoscales

Antoine Khater
Department of Physics, Le Mans University, France
Department of Theoretical Physics, Jan Długosz University, Poland

The transport of phononic energies at the nanoscale is of primary interest in recent years, and great deals of research work have developed this field. It is, however, useful to scrutinize occasionally the sense of the word *Nanoscale* because it covers significant differences in the size of systems of scientific interest, ranging from ~ 100 nanos to ~ 0.3 nano, for different research projects in strictly the submicron regime. It is clear that for material systems characterized by a dimension of a few nanos, researchers would likely treat their vibration dynamics at the atomic scale of the crystalline nanostructures of these systems. In contrast, the study of phononic thermal transfer for systems characterized by dimensions say $\geq$ 10 nanos, would lead researchers to use the continuum strain dynamics method for theoretical analysis. I will compare here these two methodologies.

The first methodology can be seen, for example, in the theoretical studies of the Kapitza resistance. This starts by studying the effect of the strain dynamics of structural defects at a solid surface, excited by the surface scattering of bulk phonons. The Kapitza thermal conductance is calculated then across the solid-liquid Helium interface, as a function of the continuum strain dynamics of surface defects, of the statistical average of the dimensions of these surface defects, and the Debye temperature of the solid He layer bound to the solid material surface.

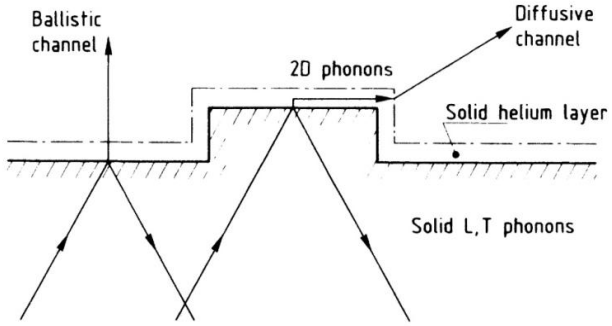

FIG. 1. Schematic representation of the ballistic and diffusive channels. The diffusive mechanism consists of flexure of the island, excitation of the 2D phonons in the solid helium layer, and their annihilation into liquid helium excitations.

The second methodology allows us, for example, to investigate the coherent phonon thermal transport on Gold nanowires, via phonon scattering at selected nanostructures on the wire. A detailed study of the transmission part under incident ballistic phonons yields the thermal conductance across the nanostructures. Using the nearest and next nearest neighbor force constants, the thermal transmission can then be calculated by the PFMT theory. The strong fluctuations of the transmission spectra are due to Fano resonances, and thermal conductance changes for different nanostructures.

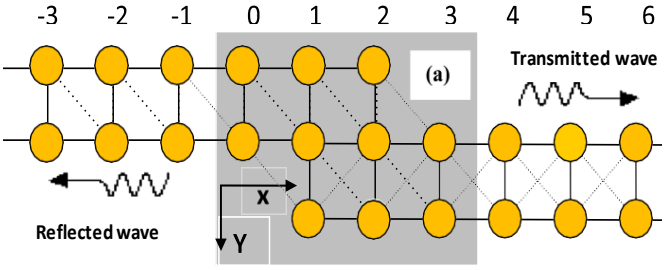

It is of interest at some point to combine these two methodologies, tested by initial efforts, toward a novel approach which can treat and continue clarifying the phononic energy transport across material systems characterized by different dimensions over the entire range of *Nanoscale*.

GDR NAME PLENIERE Rennes 2023

9-9 nov. 2023

Nanoscale Transport Properties

Extreme near field radiative heat exchange between two polar materials driven by non-optical modes

***Mauricio* Gómez Viloria**[1,*], *Yangyu* Guo[2,3], *Samy* Merabia[2], *Riccardo* Messina[1], and *Philippe* Ben-Abdallah[1]

[1]Laboratoire Charles Fabry, UMR 8501, Institut d'Optique, CNRS, Université Paris-Saclay, 2 Avenue Augustin Fresnel, 91127 Palaiseau Cedex, France

[2]School of Energy Science and Engineering, Harbin Institute of Technology, Harbin 150001, China

[3]Institut Lumière Matière, Université Claude Bernard Lyon 1, CNRS, Université de Lyon, 69622 Villeurbanne, France

Abstract.

In the near field (for separation distances smaller than the thermal wavelength, of the order of some microns at ambient temperature), the radiative heat flow between two solids at different temperatures can exceed the blackbody limit by several orders of magnitude. Furthermore, at the atomic scale, close to contact, the vibrational modes of the crystal lattice are expected to play an important role in the heat exchange. While the contribution of acoustic phonons tunneling due to Van der Waals forces and electrostatic interactions near the surface has been investigated [1–5], the radiative contribution arising from the acoustic modes has been neglected so far. Under the local assumption (wavevector $\mathbf{k} \approx 0$), optical modes are independent from the acoustic modes, and are the sole responsible for the thermal radiation for distances larger than a few nanometers. However at subnanometer distances, the electromagnetic response of solids is nonlocal ($\mathbf{k} \neq 0$) and both acoustic and optical modes are coupled, contributing together to the radiative heat exchange. In order to demonstrate the role of this contribution, we calculate [6, 7] the nonlocal dielectric permittivity of magnesium oxide (MgO) using molecular dynamics. In conjunction with near field radiative heat transfer theory, we are able to highlight the role of radiation between two polar crystals produced by acoustic modes compared to the expected results from the local theory. We show that this additional contribution can become the dominant channel for radiative heat exchanges at atomic scale in the cryogenic regime (below 100 K). Since the acoustic vibration modes can be excited with the help of piezoelectric transducers, our work opens the possibility to the control of radiative heat exchanges at atomic scale using external mechanical actuation.

*e-mail: mauricio.gomez-viloria@institutoptique.fr

References

[1] V. Chiloyan, J. Garg, K. Esfarjani, and G. Chen., Nat. Commun. **6**, 6755 (2015)

[2] J. B. Pendry, K. Sasihithlu, and R. V. Craster, Phys. Rev. B, 94 **7**, 075414 (2016)

[3] A. I. Volokitin, JETP Lett., **109**, 749-754 (2019)

[4] Y. Guo, C. Adessi, M. Cobian, and S. Merabia, Phys. Rev. B **8**, 085403 (2022).

[5] M. Gómez Viloria, Y. Guo, S. Merabia, P. Ben-Abdallah and R. Messina, Phys. Rev. B. **107**, 125414 (2023)

[6] M. Gómez Viloria, Y. Guo, S. Merabia, R. Messina and P. Ben-Abdallah, arXiv 2302.00520 (2023)

[7] Y. Guo, M. Gómez Viloria, R. Messina and P. Ben-Abdallah, S. Merabia, Phys. Rev. B **108**, 085434 (2023).

Role of dimensionality, size, and transport-direction in governing the drag Seebeck coefficient of doped silicon nanostructures.

Raja SEN[1], Nathalie VAST[1] and Jelena SJAKSTE[1*]

[1] *Laboratoire des Solides Irradiés, CEA-DRF-IRAMIS, École Polytechnique, CNRS UMR 7642, Institut Polytechnique de Paris, 91120 Palaiseau, France*

*jelena.sjakste@polytechnique.edu

Under the presence of a temperature gradient, the electric and heat currents experience a mutual drag via the coupled interaction between charge carriers and phonons [1]. The effect of phonon-drag on the charge carriers leads to significant enhancement of the Seebeck coefficient of materials [1] and therefore presents a potential interest for thermoelectric devices. However, the magnitude of phonon-drag, which in turn depends on the strength of carrier-phonon coupling and on the value of out-of-equilibrium phonon populations, has been found to diminish with nanostructuring. To engineer the phonon-drag mechanism at nanostructures, a detailed understanding of the dependence of the drag Seebeck coefficient on the dimensionality and size of nanostructures is necessary and this can only be achieved through theory because of the impossibility to separately measure the diffusion and drag contributions. We will present the recent results of our systematic investigation of the influence of dimensionality, size reduction, and heat-transport direction in governing the drag Seebeck coefficient of doped silicon nanostructures [2]. For studying the phonon-drag effect, we solved the partially coupled Boltzmann transport equations for the charge carriers and phonons, using a full ab initio description of carrier-phonon [3] and phonon-phonon interactions [4] and including the effect of phonon out-of-equilibrium populations that arise in the presence of a temperature gradient. To our knowledge, this is the first attempt at such a study that focuses on quantifying the phonon drag contribution in silicon nanostructures at various doping levels and temperatures by accounting for the anisotropy of the nanostructures (Fig.1, left panel) and the spin-orbit coupling for holes. Our results have been found to show an excellent agreement with the recent experimental findings of Refs. [5], concerning the impact of phonon-boundary scattering on the Seebeck coefficient of doped silicon nanowires (Fig. 1, right panel).

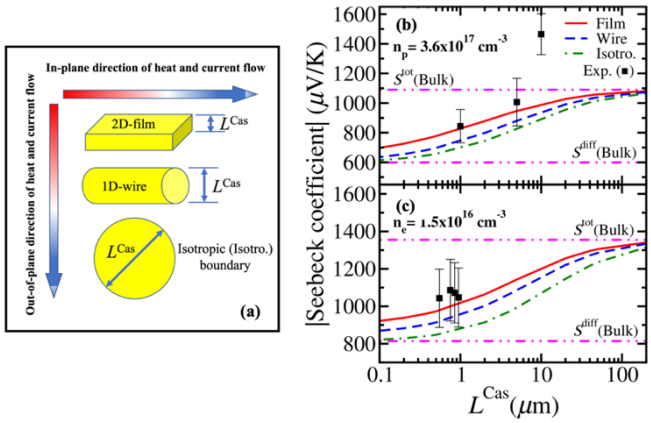

FIGURE 1. (Left panel): Schematic diagram shows the in-plane and out-of-plane direction of heat and current flow in the examined nanostructures. Right panel: Variation of the total Seebeck coefficient as a function of the silicon nanostructure size (L^{Cas}) at 300 K. Experimental data are from Refs. [5].

REFERENCES

[1] L. Gurevich, J. Phys. Moscow 9, 477 (1945), T. H. Geballe and G.W. Hull, Phys. Rev. 98, 940 (1955).

[2] R. Sen, N. Vast, J. Sjakste, Phys. Rev. B 108, L060301 (2023).

[3] J. Sjakste *et al.*, J. Phys.Condens. Matter 30, 353001 (2018), R.Sen *et al*, Appl. Phys. Lett. 120, 082101 (2022).

[4] L. Paulatto *et al.*, Phys. Rev. B 87, 214303 (2013), G. Fugallo *et al.*, Phys. Rev. B 88, 045430 (2013).

[5] K. Fauziah *et al.*, AIP Adv. 10, 075015 (2020), N. Bennett *et al.*, Appl. Phys. Lett. 107, 013903 (2015).

Thermal mass transport mechanism of an adatom on a crystalline surface

Aurélien ROUX[1,2,*] and Nicolas COMBE[1,2]

[1] *CEMES, UPR 8011, 29 rue Jeanne Marvig 31400 Toulouse*

[2] *Université Paul Sabatier, 118 route Narbonne, 31400 Toulouse*

*auroux@cemes.fr

A thermal gradient can drive the diffusion of particles inducing their motion towards the cold or hot regions. This phenomenon referred as thermomigration occurs in gases, liquids, or solids. Recent experiments have evidenced the role of thermomigration at the surface of solids [1,2]. However, the underlying physical process of thermomigration is still largely understood. In this study, we numerically and theoretically investigate the thermomigration of an adatom on a surface subjected to a temperature gradient. We restrict our research to substrates where phonons are responsible for the thermal transport. We propose a formalism for the thermomigration and show the good agreement between its prediction and outcomes of molecular dynamics (MD) simulations.

More precisely, we show that the motion of the adatom is governed by a thermodynamic potential. Through the extension of the thermodynamic integration algorithm, we compute this thermodynamic potential in MD simulations. Examining this thermodynamic potential, the thermal-gradient-induced effect is decorrelated from the stochastic diffusion. Based on these findings, we create a model for the diffusion of an adatom in this potential. Generalizing the transition state theory to an adatom in a potential subjected to a thermal gradient, we evaluate the average drift velocity of the adatom. Comparisons of this model with trajectories of MD simulations show an excellent agreement [3].

This investigation leads us to the conclusion that the main driving force for the thermomigration is the so-called intrinsic effect, i.e., the rise of the probability of presence $\propto \exp(Q/T)$ of the adatom with the decrease of temperature, where Q is found to be mainly independent of temperature and related to the adatom's binding energy to the substrate.

REFERENCES

[1] F. Leroy et al. to be published Phys Rev. Lett. (2023)

[2] DG. Xie et al., Nature communications, 10, 4478 (2019)

[3] A. Roux and N. Combe, Phys Rev. B, 108, 115410 (2023)

Thermoeletric ability of Organo(metallic) Molecular Junctions

Joseane Santos ALMEIDA [1,*], Karine COSTUAS [1] and Jérôme CORNIL [3]
[1] *Institute of Chemical Sciences of Rennes, CNRS, University of Rennes, France*
[2] *Chemistry of Novel Materials, FNRS, University of Rennes, Belgium*

*Joseane.almeida@univ-rennes1.fr

I. Introduction

Molecular Junctions (MJ) [1] can promote applications like conducting wires [2], switches [3], and sensors [4] at the nanoscale. The presence of metals in organometallic systems makes the frontier orbitals closer to the Fermi level, leading to highly conductive molecular wires [5] and increase the Seebeck coefficient for thermoelectric applications [6]. The aim of this work is to obtain good Seebeck coefficient by including a metal atom in the molecule. QuantumATK [7] simulations were performed to tackle the question using NEGF transport calculation with DFT + GGA rev-PBE/DZP and SZP for Au.

II. Fe-II and Fe-III

Fe-cyclam can be stable in two oxidation states (neutral and +1) corresponding to +II and +III Fe formal oxidation state. The Fe-III cyclam is charged and **simulate a charged MJ is a challenge**.

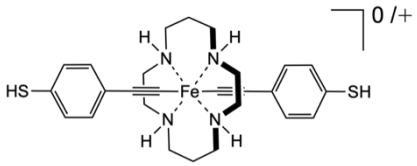

Fe^{II}(cyclam) or Fe^{III}(cyclam)

III. Partial results

A. Including a metal atom, Fe, gives high figure of merit ZT (~0.5) for Fe-II cyclam system

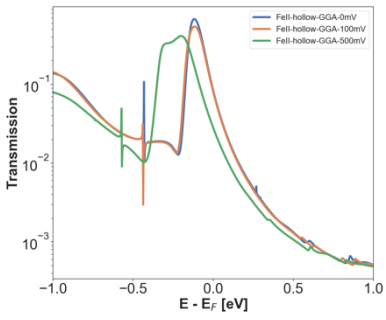

Figure 2. Electronic transmission for Fe-II cyclam MJ.

B. Include Bromine as counter ion with an energy shift in its orbitals is necessary to promote a charged molecular junction with Fe-III cyclam. Its position and shift value is carefully chosen based on mulliken population analysis.

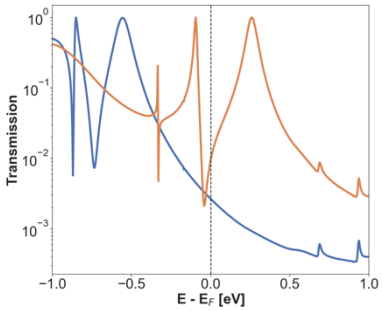

Figure 2. Electronic transmission for spin up (blue) and down (orange) for Fe-III cyclam MJ at zero bias.

- In this work, molecular junctions presenting enhanced thermoelectricity designed by a computationally-assisted molecular design. Further investigations are necessary for Fe-III cyclam to minimize the interactions between the counter ion and molecule. Furthermore, a comparison with experimental results will also be provided.

References

[1] Aviram, A.; Ratner, M.A. "Molecular rectifiers". *Chem. Phys. Lett.* 29 (2), 277-283, 1974
[2] Schwarz F et.al. "High-Conductive Organometallic Molecular Wires with Delocalized Electron Systems Strongly Coupled to Metal Electrodes." *Nano Lett*. 14, 5932−5940, 2014.
[3] Meng, F. et.al. "Photo-modulable molecular transport junctions based on organometallic molecular wires" *Chem. Sci*., 3, 3113-3118, 2012.
[4] Baghernejad, M. et.al. "Quantum Interference Enhanced Chemical Responsivity in Single-Molecule Dithienoborepin Junctions" *Chem.Eur. J.*, 25,15141-15146, 2019.]
[5] Tanaka, Y. et.al. "Inorganic and Organometallic Molecular Wires for Single Molecule Devices" *Chem.Eur. J*. 23, 4741-4749, 2017
[6] Park, S. et.al. "High Seebeck Coefficient Achieved by Multinuclear Organometallic Molecular Junctions". *Nano Lett*. 22,9693-9699, 2022
[7] S. Smidstrup et al. QuantumATK : an integrated platform of electronic and atomic-scale modelling tools. *Phys. Condens. Matter*. 32, 015901, 2020.

Temperature-induced revolving effect of electron flow in semiconductor heterostructures

C. BELABBAS[1], A. CREPIEUX[2], N. CAVASSILAS[1], F. MICHELINI[1], X. ZHU[3], C. SALHANI[3,4], G. ETESSE[1], K. HIRAKAWA[3,4], and M. BESCOND[1,3*]

[1] *IM2NP UMR-CNRS, Aix Marseille Université, Université de Toulon, Marseille, France.*
[2] *Aix Marseille Univ, Université de Toulon, CNRS, CPT, Marseille, France*
[3] *Institute of Industrial Science, University of Tokyo, Japan*
[4] *LIMMS-CNRS, IRL 2820, Tokyo, Japan.*

*marc.bescond@cnrs.fr

***Abstract*— We theoretically report a remarkable boomerang effect of electron flow when applying a lattice temperature gradient across an asymmetric double-barrier heterostructure.**

I. INTRODUCTION

Thermoelectric devices consist in converting heat into electricity or vice versa. Those devices are based on the diffusive phonon and electron transport, and operate in close to equilibrium regime, where their produced power is obviously limited. The scenario is significantly different in nanostructures where carrier transport can be assumed as strongly ballistic. In this non-equilibrium regime, electron temperature may significantly differ from the lattice one, raising the opportunity to obtain devices with better performances than conventional thermoelectric structures. We recently demonstrated that an asymmetric double-barrier heterostructure can efficiently act on both the electronic and phononic bath's refrigeration when applied a bias between the emitter and collector contacts [1].

II. MODEL AND DISCUSSIONS

Here, we focus on the opposite effect, *i.e.* when a temperature gradient is applied between the collector and the emitter, and we study the induced electrical current properties (Fig. 1). We demonstrate that electrons are subject to an unexpected revolving effect. Depending on the lattice temperature increase/decrease, electrons respectively absorb/emit a phonon and subsequently go back to the reservoir from which they have been injected (Fig. 2).

Our simulation code, which self-consistently solves the non-equilibrium Green's function framework and the heat equation, is capable to calculate the electron temperature and electrochemical potential inside the device. By investigating those non-equilibrium thermodynamic quantities (Fig.3), we show that the revolving effect is due to the sign inversion of the local electron distribution (Fig. 4). In particular, simulation results evidenced a variation of the electrochemical potential inside the device to compensate the temperature gradient, and to maintain the electrostatic neutrality in the access regions [2].

III. CONCLUSION

We report an original temperature gradient induced boomerang effect, able to control the direction flow of electrons in a given energy interval. Such a revolving effect, while it does not (almost) transport electrons, transfers a high energy flux from a hot area to a colder one. Moreover, current-voltage characteristics at different temperature gradients should be a straightforward approach to experimentally verify this effect. Finally, our study demonstrates an additional validation of the virtual probe approach to determine thermodynamic properties in strongly non-equilibrium regime.

ACKNOWLEDGMENT

This work was supported by the JSPS KAKENHI (JP 19K21957), the JSPS Core-to-Core Program (A. Advanced Research Networks), the GELATO project from ANR (ANR-21-CE50-0017) and AMUtech Institute of Aix-Marseille University.

REFERENCES

[1] M. Bescond, G. Dangoisse, X. Zhu, C. Salhani and K. Hirakawa, "Comprehensive analysis of electron evaporative cooling in double-barrier semiconductor heterostructures," *Phys. Rev. Appl*. vol.17, p.014001, 2022.

[2] C. Belabbas, A. Crépieux, N. Cavassilas, F. Michelini, X. Zhu, C. Salhani, G. Etesse, K. Hirakawa, and M. Bescond, "Temperature-induced revolving effect of electronic flow in asymmetric double-barrier semiconductor heterostructures," *Phys. Rev. Appl*. vol.20, p. 014056, 2023.

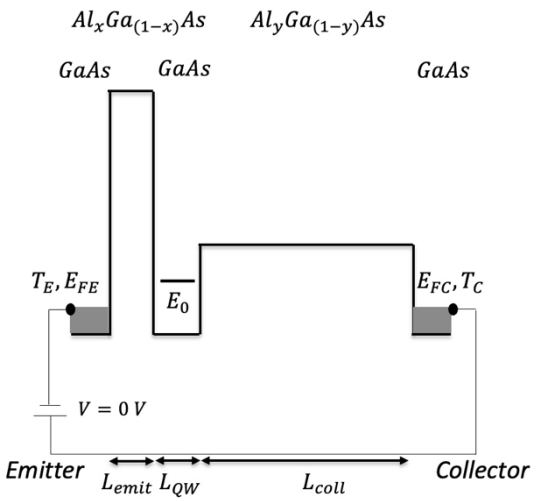

FIGURE 1: Sketch of the considered asymmetric double-barrier heterostructure. L_{emit}, L_{QW} and L_{coll} refer to the thicknesses of the emitter barrier, the quantum well and the collector barrier respectively. E_0 is the quantum well state, while E_{FE} (T_E) and E_{FC} (T_C) are the Fermi levels (temperatures) of the emitter and collector respectively. For all the considered devices, doping in the emitter and the collector is 10^{18} cm^{-3}, L_{emit}=L_{QW}=5 nm and L_{coll}=100 nm.

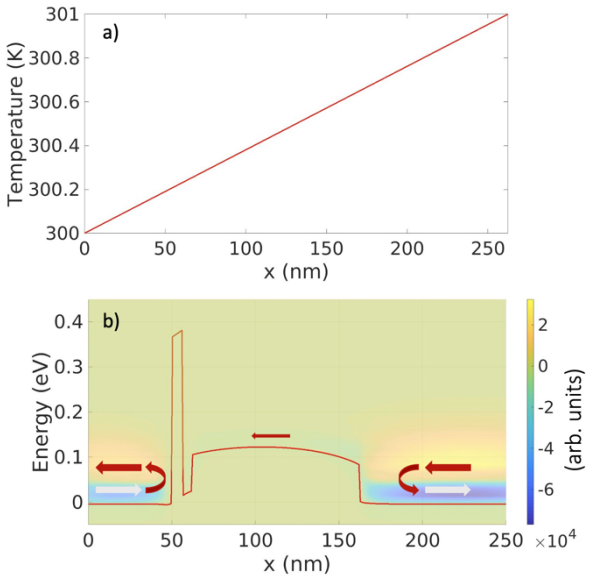

FIGURE 2: a) Lattice temperature gradient along the device shown in Fig. 1. A temperature gradient of 1 K is applied between the emitter (T_{emit}=300 K) and collector (T_{coll}=301 K) reservoirs; b) Corresponding electron current spectrum. The solid red line represents the energy potential profile, while red and white arrows indicate the electron flow and reflection on the potential barrier. The smaller red arrow in the central region represents the total electron flow, going from right to left. No potential bias is applied (V=0 V).

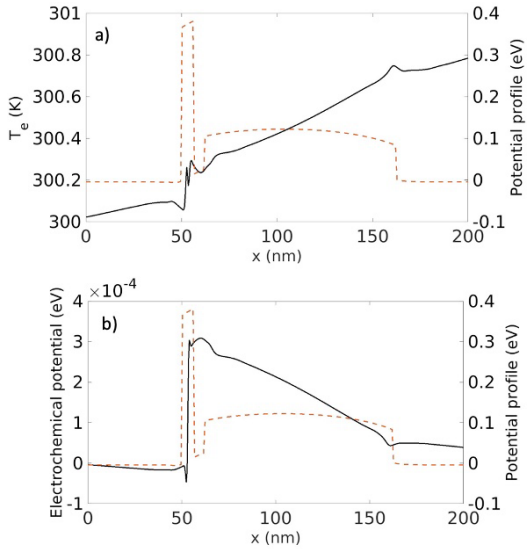

FIGURE 3: a) Non-equilibrium electron temperature along the device and b) corresponding electrochemical potential when applying lattice temperature gradient of 1 K and no potential bias (V=0 V).

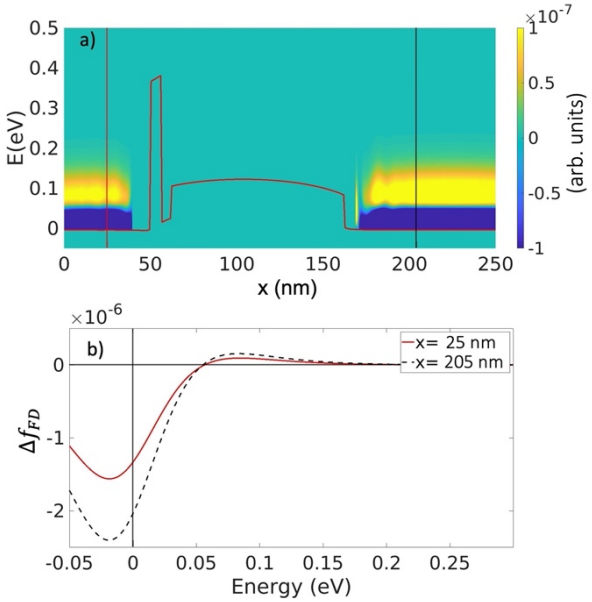

FIGURE 4: a) Difference between two consecutive plans of the Fermi-Dirac distributions calculated with the electron temperature and chemical potential shown on Fig. 3-a) and -b) respectively; b) Vertical cuts of Fig. 4-a) at x=25 nm (red solid line) and x=205 nm (dashed line). The vertical black solid line defines the Fermi-levels of the emitter and collector (equal to each other since there is no applied bias).

Thermal transfer at crystalline-amorphous interfaces: A molecular dynamics study

Julien El Hajj[1,*], Gilles Le Doux[1] and Samy Merabia[1]

[1] *Univ Lyon, Univ Claude Bernard Lyon 1, CNRS, Institut Lumi`ere Mati`ere, F-69622, VILLEURBANNE, France*

*julien.el-hajj@univ-lyon1.fr

Gold core-shell nanoparticles have demonstrated remarkable potential in various biological applications. This study focuses on investigating the interfacial thermal conductance between gold and two different materials, namely silicon and silica in both their crystalline and amorphous structures, using non-equilibrium molecular dynamics. The aim is to understand and quantify the thermal transport at the interfaces by analyzing the modal contributions to heat conduction. The findings reveal that the interfacial thermal conductance between amorphous structures and gold is significantly higher compared to crystalline structures. This observation can be attributed to the comprehensive analysis of the modal contributions and the influence of interatomic spring stiffness and cross-correlations of low frequency phonons at the interfaces.

I. Introduction

Laser heated gold nanoparticles have been widely used in terms of medicine due to the large biological applications at different scales. Considering a core-shell nanoparticle may be beneficial for many applications since silica coating on a gold nanoparticle facilitates heat transfer from the nanoparticle to its surrounding liquid [1], as well as considering a core-shell nanoparticle can increase its radiation absorbance in the near infrared region [2]. Despite the high importance and widespread use of the gold-silicon and gold-silica systems, there hasn't been a thorough investigation of the interfacial thermal conductance (ITC) between these structures. Here, the ITC between gold and silicon and gold and silica is examined in light of the crystalline and amorphous structural forms of silicon and silica, where a detailed study of the microscopical quantities is presented and compared at the interfaces of the different systems.

II. Methodology

Molecular dynamics (MD) simulations are performed using the Large-scale Atomic/Molecular Massively Parallel Simulator (LAMMPS). The calculation of the ITC is performed using non equilibrium molecular dynamics (NEMD) by applying periodic boundary conditions along the x, y and z directions. In order to generate and calculate the heat flux, a temperature gradient within the system should be created. First, the entire system is equilibrated at constant temperature and pressure. Then, the system is divided into a few regions in the direction of the temperature gradient. Hot and cold baths are located in the middle of the left and right sections and are connected to the thermostat to create a temperature gradient and heat flow. The heat flux (q) and temperature gradient are averaged throughout the simulation for ITC calculation. ITC (G) is finally calculated by dividing the heat flux by the temperature jump (ΔT) and the cross-section area (A) at the interface and is given by:

$$G = \frac{q}{\Delta T \times A} \qquad (1)$$

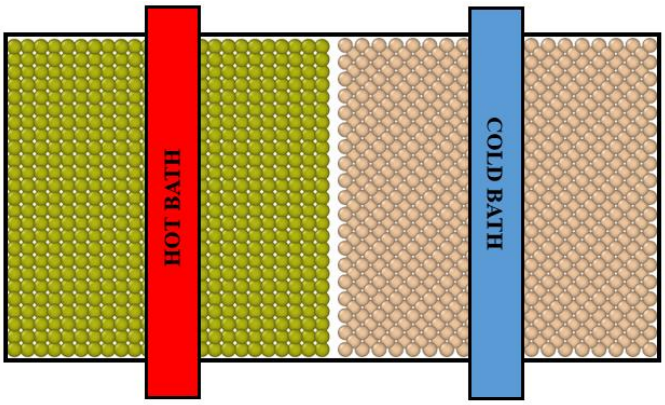

Figure 1: Schematics of the computational domain for the gold-crystalline silicon structure with its thermal baths used in the NEMD simulations to calculate the thermal conductance across the interface.

III. Results and discussion

Simulations were run for the different interfaces and the results for ITC are shown in Table 1, where ITC at the interface of gold-amorphous structures is significantly higher.

	ITC (MW/m^2 K)
Gold-crystalline silicon	56
Gold-amorphous silicon	152
Gold-crystalline silica	102
Gold-amorphous silicon	170

Table 1: Table showing the ITC computed at 300K for the four interfaces studied

The four interfaces are then compared as a function of the system size and the temperature difference between the thermal baths, and according to the calculated results, the ITC values shown in Table 1 are independent from these quantities.

Several physical quantities are computed and compared across the four interfaces in order to investigate this high increase in ITC at the gold amorphous interfaces. Going

forward, the comparison will only be between gold/crystalline silicon and gold/amorphous silicon interfaces for the sake of simplicity and since a threefold increase is observed for gold/amorphous silicon interface when compared to the gold/crystalline silicon interface. For silica, we observe qualitatively similar results.

A. Thermal spectrum

The frequency-dependent thermal flux encodes the combined information on potential energy and vibrational density of states. In the context of interfacial heat transfer, it refers to the heat flux transferred between two adjacent materials as a function of phonon frequency, which may indicate the dominant frequency range responsible for this increase.

The frequency-dependent thermal flux is defined as [3]:

$$q(\omega) = \frac{2}{A}\mathbf{Re}[\sum_{i\in Au}\sum_{j\in Si}\int_0^{t_{\max}}\langle F_{ij}(\tau)\cdot v_i(0)\rangle e^{i\omega\tau}d\tau] \quad (2)$$

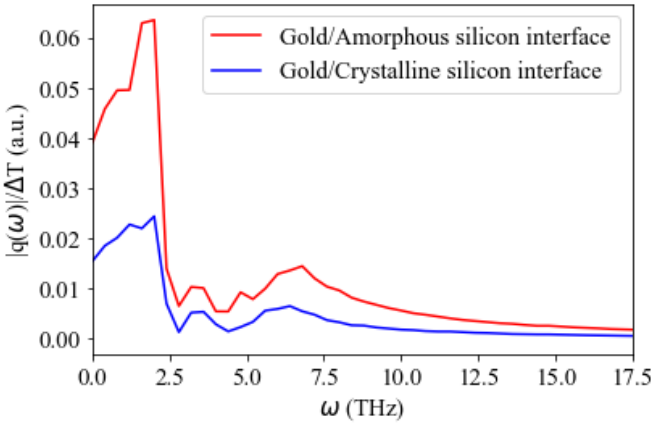

Figure 2: Frequency-dependent thermal flux at the gold/crystalline silicon and gold/amorphous silicon interfaces calculated using (2).

From Figure 2, it is seen that for both interfaces, low frequency phonons are responsible for the enhanced heat transfer. Additionally, the contribution of the low frequency phonons at the crystalline-amorphous interface is significantly higher than that at the crystalline-crystalline one.

Based on this result, the phonon modal participation ratio is calculated based on the eigenvalues and eigenvectors of the dynamical matrix at each system's interface [4]. In fact, only low frequency phonons are populated at both interfaces, and these phonons are strongly localized at the interface with a small participation ratio for the calculated frequencies.

B. Spring stiffness and atomic displacement cross-correlations thermal spectrum

We attempted to relate the thermal spectrum to the phonon spring stiffness at the interface as well as the atomic displacements of atoms in order to explain this increase in ITC. The thermal spectrum can be written as follows:

$$F(\omega) = \frac{-i\omega}{2}[\sum_{i\in Au}\sum_{j\in Si}\overleftrightarrow{K}_{ij}\langle\tilde{\vec{\Delta}}_{ij}(\omega)\cdot\tilde{\vec{\Delta}}^*_{ij}(\omega)\rangle] \quad (3)$$

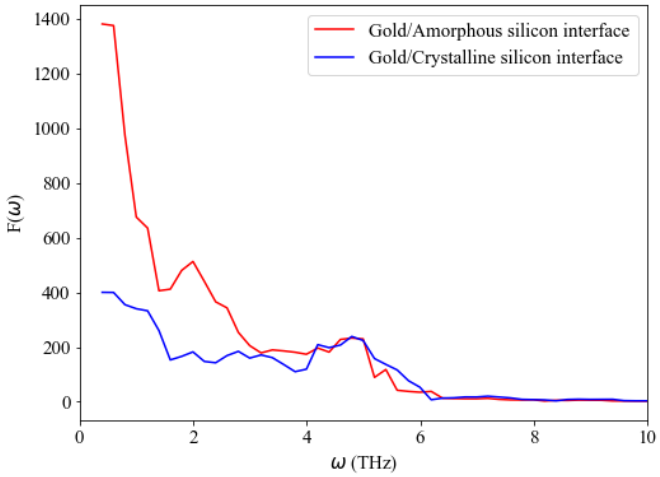

Figure 3: Frequency-dependent spring stiffness and atomic displacement cross-correlations thermal spectrum at the gold/crystalline silicon and gold/amorphous silicon interfaces calculated using (3).

Figure 3 clearly shows that low frequency modes are indeed responsible for heat transfer at both interfaces, and that the intensity is solely determined by the spring stiffness of interfacial phonons and the atomic displacement at the interfaces.

IV. Conclusion

We investigated the interfacial thermal conductance at the crystalline or amorphous silicon and silica interface with gold using MD simulations. We reported a significant increase in interfacial thermal conductance at gold-amorphous interfaces and showed that this result is driven by enhanced bonding and atomic displacement cross correlations of low frequency phonon modes at the interfaces. This study calls for the experimental investigation of interfacial thermal conductance at metal-amorphous solids.

References

[1] Chen YS, Frey W, Kim S, Kruizinga P, Homan K, Emelianov S. Silica-coated gold nanorods as photoacoustic signal nanoamplifiers. Nano Lett. 2011 Feb 9;11(2):348-54.

[2] Zhenpeng Qin and John C. Bischof. “Thermophysical and biological responses of gold nanoparticle laser heating”. In: Chem. Soc. Rev. 41 (3 2012)

[3] K. Sääskilahti et al. “Spectral mapping of heat transfer mechanisms at liquid-solid interfaces”. In: Phys. Rev. E 93 (2016)

[4] Davide Donadio and Giulia Galli. “Atomistic Simulations of Heat Transport in Silicon Nanowires”. In: Phys. Rev. Lett. 102 (2009).

Energy Conversion

Oxidized detonation nanodiamonds for the production of hydrogen under solar irradiation

Hugues A. Girard[1*], Clément Marchal[2], Lorris Saoudi[1], Valérie Keller[2], Jean-Charles Arnault[1]
[1] *Université Paris-Saclay, CEA, CNRS, NIMBE, 91191 Gif sur Yvette, France*
[2] *ICPEES, CNRS/University of Strasbourg, UMR 7515, 67000 Strasbourg, France*
*hugues.girard@cea.fr

***Abstract*—In this paper, we evidence that oxidized detonation nanodiamonds (Ox-DND) can produce hydrogen under solar irradiation without addition of co-catalyst or formation of heterojunction with another semiconductor. At its maximum, a H_2 production yield of 32 µmol.h^{-1} was measured for a Ox-DND concentration of 12.5 µg/mL (using only 1 vol.% of TEOA as sacrificial reagent), similar to the one of TiO_2 nanoparticles tested at the same concentration in the same illumination conditions.**

Compared to other nanoscale semiconductors, nanodiamond (ND) has not been really considered for photocatalytic reactions. This originates from the confusion with ideal monocrystalline diamond behaving a wide bandgap (5.5 eV) that requires deep UV illumination to initiate photoreactivity. At nanoscale, diamond particles enclose native defects that create energetic states decreasing the light energy needed to initiate charge separation. This is supported by recent studies that involved our group with experimental results and DFT calculations [1]. The presence of sp2 carbon in hydrogenated detonation ND allows the emission of solvated electrons in water under visible light (400 nm) according to ultrafast transient absorption spectroscopy. In addition, the diamond electronic structure can be strongly modified playing on its surface terminations (oxidised vs hydrogenated) [2]. Combining these assets, ND becomes competitive to other semiconductors toward photoreactions. Its potential needs to be deeply investigated.

In this context, this study reports on the photocatalytic H_2 production from water using ND alone under broad and moderate solar illumination conditions. We used Detonation nanodiamonds (DND), oxidized by an annealing in air leading to a predominance of carboxylic groups on their surface, and suspended in water. These particles also exhibited some sp^2 carbon reconstructions at their surface according to XPS and Raman spectroscopy. H_2 measurements were realized in dynamic mode, under N_2 flow (100 cc/min), in presence of a hole scavenger (1 vol.% TEOA) and sun-like illumination. P25 TiO_2 nanoparticles (Evonik) were studied under similar conditions as reference. After 50 min of stabilization, formation rate of H_2 reaches almost 3000 µmol.h-1.g-1, which is comparable to P25 TiO_2. Such effect is not observed for hydrogenated DND from the same source. H_2 production with oxidized DND was also evidenced in presence of methanol as hole scavenger. This study evidences the positive impact of ND for photocatalytic H_2 production by water-splitting without the addition of noble metal co-catalyst and with low amount of sacrificial agent (below or equal to 1 vol.%).

REFERENCES

[1] F. Buchner, T. Kirschbaum, A. Vérénosy, H. Girard, J.-C. Arnault, B. Kiendl, A. Krueger, K. Larsson, A. Bande, T. Petit, C. Merschjann, Nanoscale. 2022, 14, 17188.

[2] C. Nebel, Nature Materials. 2013, 12, 780.

Laser synthesized nanoparticles for reduction or oxidation reactions.

Guillaume DUBOIS[1], Fabien GRASSET[2], Corinne LAGROST[1], Suzy SURBLE[4], Pierre LONCHAMBON[4], Tetsuo UCHIKOSHI[2,3], Franck TESSIER[1], Xiaoyong MO[5], Edmund C.M. TSE[5], Nathalie HERLIN BOIME[4*],

[1] *Univ. Rennes, CNRS, UMR6226-ISCR, Rennes, France ;*
2 LINK, IRL3629 CNRS-Saint-Gobain-NIMS, NIMS,Tsukuba, Japan;
3 NIMS, Tsukuba, Japan,
[4] *CEA, IRAMIS, UMR3685 NIMBE, Univ. Paris Saclay, Gif-sur-Yvette, France*
[5] *Department of Chemistry, HKU-CAS Joint Laboratory on New Materials, University of Hong Kong, Hong Kong SAR, China*

*Nathalie.Herlin@cea.fr

Transition metal carbides and nitrides demonstrate very interesting electrocatalytic properties, close to those of noble metals.[1,2] Indeed, platinum being a scarce and expensive element, carbides and nitrides could be an interesting alternative to make this technology economically viable.

In this context, carbides or (oxy)nitrides nanomaterials were synthesized using the Laser pyrolysis method. This gas phase method offers several advantages, it is versatile and allows using gaseous or liquid reactants for the one step production of nanoparticles. It is based on the interaction of Laser beam and a precursor and leading to the s production of high purity nanoparticles. It has already been developed at industrial scale (see for example www.nanomakers.fr).

Recently, different authors have reported promising electrocatalytic properties of molybdenum carbides for the HER reaction.[3,4,5]. In the present case, molybdenum carbides or (oxy)nitrides directly mixed with graphitic carbon (GC) in the form of nanocomposites, noted MoyXz/GC, X = C, N) were obtained from commercial molybdenum sources. The solid precursor of molybden nitrate was dissolved in water and introduced in the Laser beam as liquid droplets. After heating by the Laser beam, evaporation of droplets occurs followed by nucleation and growth of nanoparticles. The resulting materials were characterized with several complementary techniques (XRD, SBET measurement, SEM, etc.)[6]. These compounds show some activity for HER reaction.

Using the same method, various compositions of tantalum-based nanomaterials were synthesized and used as bifunctional catalysts for direct peroxide-peroxide Fuel Cells[7]. Indeed, by varying the laser power, reactor parameters, and ammonia flow rate, five Ta/N/O nanomaterials are prepared containing Ta_2O_5, Ta_4N_5, Ta_3N_5, and TaN in tunable ratios. Electrochemical studies in neutral and alkaline conditions demonstrate that Ta_4N_5 is the active component for H_2O_2 oxidation and reduction. Kinetic isotope effect (KIE) studies show that protons are involved at or before the rate-determining step (RDS). Long-term stability studies indicate that Ta_3N_5 grants Ta/N/O nanomaterials their enhanced longevity during electrocatalytic operations. Taken together, Ta/N/O can act as active and robust electrocatalysts for H2O2 reduction and oxidation. Laser pyrolysis is envisioned to produce refractory metal nanomaterials with boosted corrosion resistance for energy catalysis

REFERENCES

1) Hargreaves, J. S. J. et al. Coord. Chem. Rev. 257, 2015-2031 (2013).
2) Wang, H. et al. Chem. Soc. Rev. 50, 1354-1390 (2021).
3) Wan, C. et al. Angew. Chem. 126, 6525-6528 (2014).
4) Kumar, R. et al. J. Mater. Chem. A 5, 7764-7768 (2017).
5) Gujral, H.S. et al. Sci. Technol. Adv. Mater. 23, 76-119 (2022).
6) Caroff, T. et al. Nanomanufacturing 2, 112-123 (2022)
7) Mo, X. et al. SmartMat, (2023) DOI10.1002/smm2.1181

Surface modified epitaxial GaAs|Si for solar H_2 production

Hanh Vi LE[1,*], Mekan PIRIYEV[1], Sylvain FEBVRE[1,3], Gabriel LOGET[2], Bruno FABRE[2], Sylvie HAREL[4], Angus ROCKETT[5], Kenneth STEIRER[5], Tony ROHEL[1], Karine TAVERNIER[1], Julie LE POULIQUEN[1], Ludovic LARGEAU[6], Gilles PATRIARCHE[6], Rozenn BERNARD[1], Yoan LÉGER[1], Nicolas BERTRU[1] and Charles CORNET[1]

[1] *Univ Rennes, INSA Rennes, CNRS, Institut FOTON-UMR 6082, F-35000, Rennes, France.*

[2] *Univ Rennes, CNRS, ISCR (Institut des Sciences Chimiques de Rennes) -UMR6226, Rennes F-35000, France.*

[3] *3SP Technologies SAS, 91625 Nozay, France.*

[4] *Institut des Matériaux Jean Rouxel (IMN) CNRS UMR6502, 2 rue de la Houssinière BP 32229, 44322 Nantes Cedex3, France.*

[5] *Department of Metallurgical and Materials Engineering, Colorado School of Mines, 1500 Illinois St., Golden, Colorado 80401, United States.*

[6] *Center for Nanoscience and Nanotechnology, C2N UMR 9001, CNRS, Université Paris Sud, Université Paris Saclay, Palaiseau, France.*

*corresponding author e-mail

***Abstract*—GaAs is an excellent candidate for high performance photocatalysis due to its appropriate band edge energies and its transport properties. The most significant limitations of GaAs for photoelectrochemical (PEC) applications are the instability against corrosion, high substrate cost and huge overpotentials. We present here a strategy that can overcome these challenges. We developed photocathodes made of 1 µm-thick molecular beam epitaxy (MBE) grown GaAs layer on p-Si substrates and compared their performance to that of bare p-GaAs electrodes. Passivation and catalytic properties were analyzed for both series of photocathodes. The maximum photocurrent density was obtained at 0 V vs Reversible Hydrogen Electrode (RHE) (expected working potential for an autonomous PEC cell) and a high photocurrent onset potential (V_{onset}) of 0.4 V vs RHE was demonstrated for GaAs/Si sample after Pt deposition and S-passivation, even better than the values of the GaAs wafer. A long-term stability of our sample of more than 112 hours was also demonstrated. These findings provide guidance for further studies towards the fabrication of stable unassisted PEC cells for green hydrogen production.**

I. INTRODUCTION

One of the most important problems facing humanity nowadays is the production and storage of clean, renewable, and low-cost energy. Solar PEC H_2 production could potentially meet the above criteria, through the direct conversion of solar energy into H_2. From the band line-up for selected semiconductors [1], GaAs is shown to have suitable band positions for Hydrogen Evolution Reaction (HER). The stability of GaAs photoelectrodes has been investigated in the literature and the results suggest that GaAs undergoes active corrosion under anodic conditions[2], [3], while GaAs photocathodes are rather stable [4], [5]. GaAs is a promising material, but its high overpotential is still one of the most significant drawbacks that we must overcome. Dealing with surface recombination and catalytic effects is one solution. Several studies on the passivation and catalytic performance of p-GaAs have been conducted but these two processes are still not well understood. It has been shown that catalyst deposition on p-GaAs can shift V_{onset} to a more positive value[4], [6]–[8]. Several papers have shown the catalytic effects of Pt deposited by different methods such as: sputtering, electrodeposition, electroless deposition, electron beam deposition on p-GaAs. Some of them claim that Pt deposition on GaAs surface creates elemental As which produces mid-gap surface states hence badly affects the quality of the photocathodes [4]. Others state that a positive shift in V_{onset} can be expected since Pt is a good catalyst for hydrogen evolution [6], [8]. But in all cases, the best V_{onset} obtained was 0.25 V vs RHE [7]. In addition, it has been extensively reported that using S-passivation on III-V materials can reduce surface states [9]. However, relatively few studies have been published about the effects of S-passivation on electrochemical applications [10]. The effects of passivation and catalysts on the performance of GaAs photocathodes must therefore still be deepened. In this work, we developed simple and cost-efficient structures based on epitaxial GaAs/Si and investigated the effects of catalytic Pt and S-passivation on these structures. Samples with Pt deposition followed by S-passivation show the best performance with a maximum V_{onset} of 0.4 V vs RHE and large stability. This is the first time a cost-effective sample exhibits such a high V_{onset}, even better than the one of GaAs photocathodes. In the following, we present the fabrication and surface preparation of our electrodes as well as their compositional, structural and surface characterizations and PEC properties.

II. EXPERIMENTAL SECTION

P-GaAs (100) substrates (Zn-doped, 0.72-2.8 × 10^{17} cm^{-3}, commercial sources) and 1 µm thick GaAs (non-intentionally doped) grown by MBE on p-Si substrates (10^{16} cm^{-3}, 6° off) were used as light absorber. Ohmic back contact was formed using Ga-In eutectic and silver paste.

A. Electrochemical characterization

Three-electrode PEC cell was used, with samples as the working electrode, a graphite rod as the counter electrode and an Ag/AgCl as the reference electrode. Electrolyte used was H_2SO_4 0.2 M. All measurements were performed at room temperature and were conducted under AM1.5G.

B. Platinum electroless deposition

Samples were dipped in HF 4.6 M solution and H_2PtCl_6 1 mM for 10 seconds. Samples were then rinsed with ultra-pure water and dried under a N_2 stream.

C. Sulfur Passivation

Samples were dipped in HCl 10% solution for 1 minute, followed by $(NH_4)_2S$ 20% solution for 1 hour. After treatment, samples were dried under a N_2 stream.

III. Results and Discussion

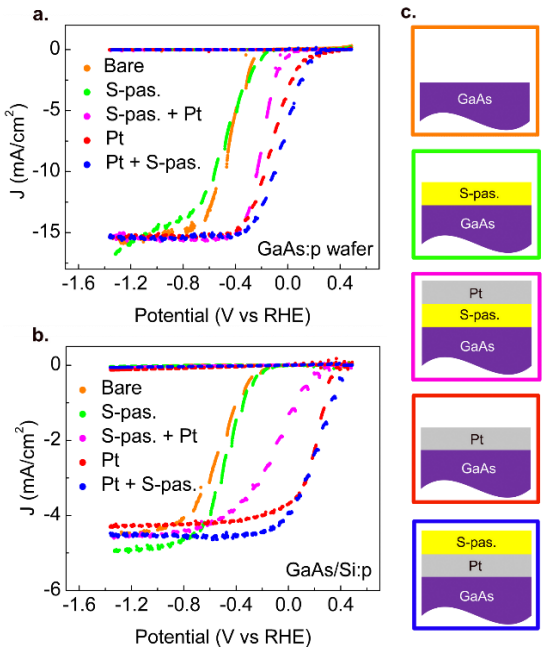

FIGURE 1. a) Current density-potential (J-V) curves of GaAs photocathodes at various material configurations, including bare GaAs, GaAs with S-passivation, GaAs with S-passivation and Pt. b) J-V curves of GaAs/Si photocathodes with the same configurations as in a. c) Sampleconfigurations with color codes consistent with J-V curves in a and b.

Fig. 1 shows J-V curves of GaAs and GaAs/Si based-photocathodes with different surface preparations. Photocurrents of GaAs-based photocathodes are measured at -15 mA/cm^2, higher than that of GaAs/Si based-photocathodes at -5 mA/cm^2. Their V_{onset} are comparable, near -0.2 V vs RHE. V_{onset} significantly increases in both cases when Pt is electrolessly deposited on the surfaces. A small improvement was observed after S-passivation and the best V_{onset} are obtained when Pt deposition is followed by S-passivation. We noticed that V_{onset} of GaAs/Si photocathodes improves much more compared to that of GaAs wafer photocathodes. V_{onset} of p-GaAs wafer was enhanced from -0.19 to 0.15 V vs RHE and V_{onset} of GaAs/Si is from -0.23 to 0.4 V vs RHE. This can be explained by the difference on the oxide formation on GaAs and GaAs/Si. Fig. 2a and b show XPS spectra of the peak Ga 3d of GaAs and GaAs/Si samples before and after Pt deposition. The results indicate that for GaAs, the amount of oxide increases after Pt deposition. However, a different trend is observed for GaAs/Si. This may be due to the different doping values of GaAs of the two samples. Energy Dispersive X-ray Spectroscopy (TEM-EDX) (Fig 2c) was performed on Pt/GaAs/Si after 2.5 hours in electrochemical conditions and the extracted profiles were shown in Fig. 2d. An inhomogeneous layer of Pt (~ 3 nm) is shown, explaining the efficiency of S-passivation after Pt deposition. A continuous layer of GaO_x of 3 nm below Pt layer is surrounded by As-rich layer (elemental As and AsO_x). Stability test of 112 hours was also performed for sample Pt/GaAs/Si. During the 4 first hours, photocurrent decreases from -4 to -2 mA/cm^2, then stabilized until 90 hours.

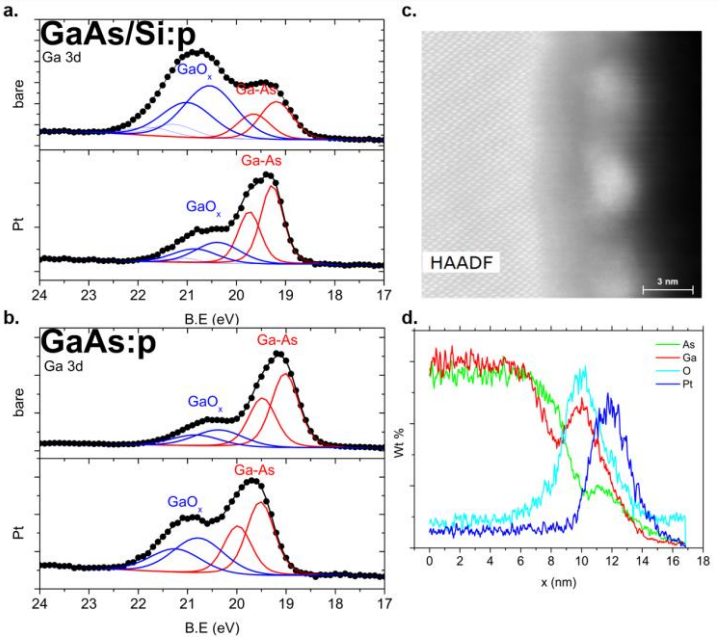

FIGURE 2. XPS spectra before and after Pt deposition of a) GaAs:p wafer b) GaAs/Si:p. c) TEM cross-section images of GaAs/Si with Pt deposition after 150 minutes in electrochemical conditions at 0 V vs RHE and d) TEM-EDX profiles measured along image c from left to right.

IV. Conclusion

In this work, we were able to analyze two processes: catalytic effects and passivation, independently. For the first time, a cost-efficient GaAs/Si sample can produce such a high V_{onset} as 0.4 V vs RHE, even better than that of the GaAs wafer. The long-term stability of GaAs/Si of more than 112 hours have been demonstrated.

Acknowledgment

This research is supported by the "France 2030" French National Research Agency NAUTILUS Project (Grant no. ANR-22-PEHY-0013).

References

[1] C. G. Van de Walle et J. Neugebauer, *Nature*, vol. 423, nº 6940, Art. nº 6940, juin 2003, doi: 10.1038/nature01665.

[2] K. Walczak *et al.*, *ChemSusChem*, vol. 8, nº 3, p. 544-551, 2015, doi: 10.1002/cssc.201402896.

[3] M. Piriyev *et al.*, *Sol. Energy Mater. Sol. Cells*, vol. 251, p. 112138, mars 2023, doi: 10.1016/j.solmat.2022.112138.

[4] W. Yu, M. H. Richter, E. Simonoff, B. S. Brunschwig, et N. S. Lewis, *J. Mater. Chem. A*, vol. 9, nº 40, p. 22958-22972, oct. 2021, doi: 10.1039/D1TA04145B.

[5] J. L. Young, K. X. Steirer, M. J. Dzara, J. A. Turner, et T. G. Deutsch, *J. Mater. Chem. A*, vol. 4, nº 8, p. 2831-2836, 2016, doi: 10.1039/C5TA07648J.

[6] M. Khader, *Int. J. Hydrog. Energy*, vol. 21, nº 7, p. 547-553, juill. 1996, doi: 10.1016/0360-3199(95)00118-2.

[7] K. Choi, K. Kim, I. K. Moon, I. Oh, et J. Oh, *ACS Appl. Energy Mater.*, vol. 2, nº 1, p. 770-776, janv. 2019, doi: 10.1021/acsaem.8b01838.

[8] S. Cao *et al.*, *Adv. Energy Mater.*, vol. 10, nº 9, p. 1902985, 2020, doi: 10.1002/aenm.201902985.

[9] M. Rebaud, M.-C. Roure, V. Loup, P. Rodriguez, E. Martinez, et P. Besson, *ECS Trans.*, vol. 69, nº 8, p. 243-250, sept. 2015, doi: 10.1149/06908.0243ecst.

[10] H. Lim, J. L. Young, J. F. Geisz, D. J. Friedman, T. G. Deutsch, et J. Yoon, *Nat. Commun.*, vol. 10, nº 1, Art. nº 1, juill. 2019, doi: 10.1038/s41467-019-11351-1.

REALISATION DE MICROELECTRODES 3D PAR VOIE LIQUIDE POUR MICROSUPERCONDENSATEUR

Nathalie POIROT[1,*], Mohamed BOUFNICHEL[2], Rachelle OMNEE[3,4]

Encarnacion Raymundo-Piñero[3,4]

[1] GREMAN, UMR7347, CNRS/Université François Rabelais, IUT de Blois, 15 rue de la Chocolaterie, 41000 Blois, France

[2] STMicroelectronics, 10 rue Thalès de Milet, 37071 Tours, France

[3]CNRS, CEMHTI UPR3079, Univ. Orléans, 1D avenue de la Recherche Scientifique, 45071 Orleans, France

[4]Réseau sur le Stockage Electrochimique de l'Energie (RS2E), Cedex FR CNRS 3459, Amiens, 80039, France

*Nathalie.poirot@univ-tours.fr

***Résumé*— Le développement de systèmes énergétiques miniaturisés et de microdispositifs sur structuration tridimensionnelle (3D) est en plein essor, notamment dans le domaine des microbatteries et microsupercondensateurs[1,2]. Les avantages de la structuration de dispositifs 3D sont : la réduction de la taille et du coût, l'augmentation de la fiabilité et de la densité énergétique stockée. Les techniques actuelles de dépôt de couches minces sur substrats 3D sont le PVD, CVD, ALD, la pulvérisation cathodique, etc...Nous proposons une nouvelle approche de dépôt de films minces homogènes sur des substrats 3D par voie liquide en trois étapes : (1) Préparation d'une solution de précurseur visqueux (2) Dépôt de solution sur la soustraction 3D par spin coating (3) Traitement thermique [3] . Les résultats des dépôts d'oxydes métalliques obtenus des substrats Si microstructurés 3D sur différentes architectures à haut facteur d'agrandissement de surface (AEF) sont montrés ainsi que leur performances propriétés électrochimiques**

I. DEPOTS CONFORMES SUR SUBSTRATS 3D

La préparation des substrats 3D de Si sont décrits dans la littérature[3]. La préparation de TiO_2 se fait par voie sol-gel [4]. 2.86 mL de tétrabutyl de titane, 0.86 mL d'acétylacétone et 1.14 mL d'eau sont mélangés. Du propanol est ajouté afin d'obtenir 20 mL de solution à une concentration de 0.42 mol.L^{-1} (sol S1). Deux autres solutions sont préparées avec la méthode décrite ci-dessus avec différente concentration de Ti (sol S2 avec une concentration de 0.21 mol.L^{-1} et sol S3 concentration de 0.105 mol.L^{-1}). La procédure de dépôt inclut l'addition d'une résine polyester aux sols S1, S2 et S3. Les mélanges résine/sol sont déposés sur des substrats de Si-3D par spin coating (SPS-Europe Spin150) [3,5]. Les dépôts sont traités thermiquement sur plaques chauffantes pour éliminer la résine et le solvent (175 °C pendant 5 min, 375 °C pendant 10 min) puis un traitement thermique de type RTA(rapid thermic annealing) à 700 °C pour cristalliser l'oxyde est réalisé.

L'utilisation des sols S1, S2, et S3, permet la formation de films minces de TiO_2 avec des épaisseurs respectives de 50 nm, 40 nm et 20 nm. Une couche d'une épaisseur de 90 nm est obtenue par un dépôt de sol S1 puis de sol S2. Pour obtenir des épaisseurs de couches de 120 nm, 200 nm, et 300 nm, le process est répété respectivement 2, 4 ou 5 fois en utilisant le sol S1.

Pour avoir un bon contact électrique, lors des mesures électrochimiques une couche de Ti de 200 nm d'épaisseur est déposée en face arrière par PVD. Des couches de TiO_2 ont été également déposées sur substrats 2D avec les mêmes épaisseurs de dépôts que sur les substrats 3D.

II. RESULTATS

Les dépôts ont été réalisés sur substrats 3D ayant des morphologies de type piliers et tranchées avec des facteurs de forme (FF : rapport de la hauteur divisée par la largeur) différents [6]. Les images MEB sont présentées figure 1 indiquent que les recouvrements sont conformes. La matière active est présente sur toute la surface du système 3D, aucune fissuration a été observée même sur les géométries avec rupture d'angle.

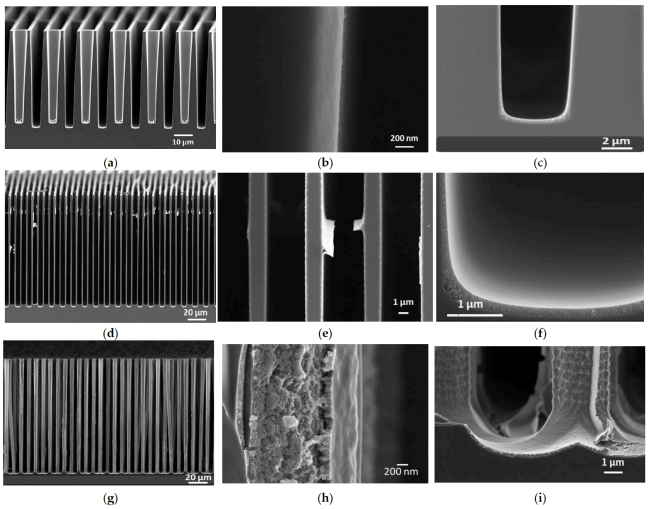

FIGURE 1 : IMAGES MEB DE LA COUCHE DE TiO_2 SUR DES TRANCHEES 3D AVEC FF 9 : (A) VUE GENERALE, (B) PAROI D'UNE TRANCHEE ET (C) FOND D'UNE TRANCHEE. IMAGES SEM DE LA COUCHE DE TiO_2 SUR DES TRANCHEES 3D AVEC FF29 : (D) VUE GENERALE, (E) PAROIS D'UNE TRANCHEE ET (F) FOND

D'UNE TRANCHEE. IMAGES MEB DE LA COUCHE DE TiO_2 OBTENUE SUR DES PILIERS 3D AVEC FF 29 : (G) VUE GENERALE, (H) PAROI DU PILIER ET (I) FOND DU PILIER.

Les études électrochimiques sont présentées sur la figure 2. Les profils CV d'électrodes (figure 2a) ayant une couche de TiO_2 de même épaisseur mais avec un support 2D ou 3D ayant un FF de 29 présentent le même profil (contribution capacitive et faradique). On peut observer les pics de réduction et d'oxydation aux mêmes potentiels. La structuration du substrat Si n'a donc aucune influence sur la nature chimique du film déposé. L'augmentation de la surface spécifique de l'électrode jusqu'à 34,4 cm^2 entraîne une augmentation de la capacité surfacique.

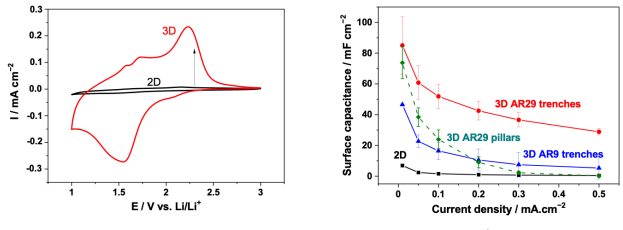

FIGURE 2 : VOLTAMOGRAMME A 1 MV S^{-1} D'ELECTRODES DE TiO_2 2D ET 3D (FF29) AYANT 120 NM DE MATERIAU ACTIF (**B**) CAPACITE SURFACIQUE POUR DES ELECTRODES 120 NM DE TiO_2 POUR DES SUBSTRATS 2D ET 3D AYANT DES MORPHOLOGIES DE TYPE TRANCHEES OU PILIERS ET DES FF DE 9, ET 29.

Cette augmentation de capacité surfacique a été observée pour des cycles galvanostatiques de charge-décharge à des densités de courant allant de 0,01 à 0,5 mA cm^{-2}.

La figure 2b montre que la topologie type tranchées permet d'accroître la capacité surfacique de façon plus significative que celle en piliers. L'électrode ayant la topologie tranchée, ayant le FF de 29 montre une capacité surfacique de 28,8 $mF.cm^{-2}$. Par conséquent, la topologie tranchées permet une amélioration simultanée de la densité d'énergie, à mesure que la capacité de surface augmente, et de la densité de puissance, répondant ainsi aux exigences d'un supercondensateur. Les différences observées entre les topologies pourraient être dues à la qualité de l'interface TiO_2/Si. Le dépôt d'une couche de nanoparticules de TiO_2 sur la surface des tranchées peut conduire à une adhérence supérieure par rapport au dépôt sur les surfaces courbes des piliers. De tels problèmes d'interface ont un impact substantiel sur les performances électrochimiques lors du fonctionnement avec des matériaux actifs peu conducteurs, tels que le TiO_2.

III. CONCLUSION

Une nouvelle approche de dépôts de couches de TiO_2 sur des substrats de Si 3D avec différents rapports d'aspect en utilisant une voie liquide et un dépôt de revêtement par spin-coating a été développée ici. Cette méthode est simple, rapide et peu coûteuse. De plus, elle pourrait être utilisée dans des applications industrielles. La méthode proposée permet d'obtenir un revêtement en couche mince de TiO_2 homogène sur des substrats 3D ayant des facteurs de forme élevés. La solution précurseur à viscosité modulée par ajout de résine, pénètre à l'intérieur des structures 3D et recouvre uniformément les parois. L'épaisseur des couches de matériau actif peut être contrôlée en modifiant la concentration de la solution et le nombre de couches déposées. Pour un matériau faiblement conducteur, tel que le TiO_2, l'épaisseur de la couche active optimale sur un support 2D s'est avérée être d'environ 120 nm. Pour un revêtement d'épaisseur similaire, une topologie de tranchée 3D du substrat augmente la capacité de surface de 27 fois à de faibles densités de courant pour atteindre une capacité de surface de 85,0 $mF.cm^{-2}$. Par conséquent, une augmentation de la surface de l'électrode est bénéfique à l'augmentation de la densité d'énergie. A des densités de courant élevées, la topologie de tranchée 3D permet d'obtenir une capacité de surface multipliée par 72 avec une valeur de capacité de 28,8 $mF.cm^{-2}$ à 0,5 $mA.cm^{-2}$. La méthode proposée pour déposer du TiO_2 sur un support à indice de forme élevé est idéale pour développer des microsupercondensateurs à haute énergie et haute puissance possédant une durée de vie prometteuse.

REMERCIEMENTS

Remerciements à David Chouteau, Virginie Grimal, Morgane Dutour et Pierre-Ivan Raynal pour leurs contributions pour le projet.

REFERENCES

[1] S. Ferrari; M. Loveridge,.S.D.Beattie, M. Jahn, R.J. Dashwood, R; R. Bhagat, Latest advances in the manufacturing of 3D rechargeable lithium Microbatteries. *J. Power Sources*, *286*, 25–46,2015

[2] C.Lethien,; J.L.Bideau, T.Brousse, T. Challenges and prospects of 3D micro-supercapacitors for powering the internet of things. *Energy Environ. Sci.*, *12*, 96–115,2019; K.H.Dinh, P. Roussel, C. Lethien, "Advances on Microsupercapacitors: Real Fast Miniaturized Devices toward Technological Dreams for Powering Embedded Electronics?" ACS Omega 2023, 8, 8977−8990, 2023

[3] N. Poirot, T. Tillocher, P.I. Raynal, Conformal coating by liquid route on three-dimensional topology. Eur. Phys. J. Spec. Top. 2022, 231, 4245–4253, 2022.

[4] M.K. Patil, S. Shaikh, I. Ganesh, Recent advances on TiO_2 thin film based photocatalytic application (A Review). *Curr. Nanosci.*, *11*, 271–285,2015

[5] A. Vincent, N. Poirot, International patent : WO/2015/044582 A1, M. Gabard *et al*., ChemEngineering 1(1), 5 (2017) N. Poirot, International patent : WO/2018/229266

[6] N. Poirot, M. Gabard, M. Boufnichel, R. Omnée, Encarnacion Raymundo-Piñero, "A suistainable approach for the development of TiO_2 based 3D electrodes for micro-supercapacitors", Batteries, 9, 258,2023.

10-10 nov. 2023

Energy Conversion

III-V Core / Oxide Shell Nanowires for Light-Driven Water Splitting

Thomas Dursap * , Philippe Regreny , Cristina Tapia , Celine Chevalier , Nicolas Chauvin , Michel Gendry , Alexandre Danescu , Matthieu Koepf , Vincent Artero , Matthieu Bugnet *

[1], Jose Penuelas * † [2]

[1] Matériaux, ingénierie et science [Villeurbanne] – Université Claude Bernard Lyon 1, Institut National des Sciences Appliquées de Lyon, Centre National de la Recherche Scientifique – France
[2] INL - Matériaux Fonctionnels et Nanostructures – Institut des Nanotechnologies de Lyon – France

Mots-Clés: Nanowires, photoelectrodes, III, V

*Intervenant
†Auteur correspondant: jose.penuelas@ec-lyon.fr

Quantum description of nano-objects for molecular solar thermal energy storage

Corentin Poidevin,[1] Carlos R. Lien-Medrano,[2] Arnaud Fihey[1]

[1] Univ Rennes, CNRS, ISCR (Institut des Sciences Chimiques de Rennes) - UMR 6226, F-35000 Rennes, France

[2] Bremen Center for Computational Materials Science (BCCMS), Universit¨at Bremen, 28359 Bremen, Germany

Email: arnaud.fihey@univ-rennes.fr

Keywords: Molecular Modeling, Solar thermal fuel, photochromism, Nanoparticle

Converting and storing efficiently solar energy is a critical challenge in chemical physics science and engineering, and constitutes a pressing issue for modern society. Among the recent answers to this question, converting light into heat through the isomerization of an organic molecule offers a promising solution, showing great potential for a number of applications such as in solar thermal storage. The so-called “Molecular solar thermal” systems (MOST) can indeed store energy from light with the help of a photochromic process. [1] Today, promising photochromic candidates for such MOST systems consist mostly in derivatives of azobenzene or the norbornadiene/quadricyclane (NBD/QC) couple. Up to today, very few works explore how the grafting onto a support impact the MOST efficiency and are mostly limited to carbon-based material. [2]

In this contribution we explore with quantum mechanics tools, hybrid nanomaterial composed of gold nanoparticles functionalized with azobenzene or NBD/QC ligands in the framework of MOST devices. To achieve such heavy computations, we make use of a parameterized Density Functional Tight-Binding (TD-DFTB) [3] method. After an exploration of the geometry of the system through Molecular Dynamics, we focus on the impact of the size of the NP and the spacer on the electronic and optical properties of the resulting hybrid systems. Characteristics of interest for the energy storage, e. g. the energy stored through isomerization, is computed and compared to the starting isolated photochrom, in order to highlight potential packing (from other grafted molecules) and electronic (from the nanoparticle) effects.

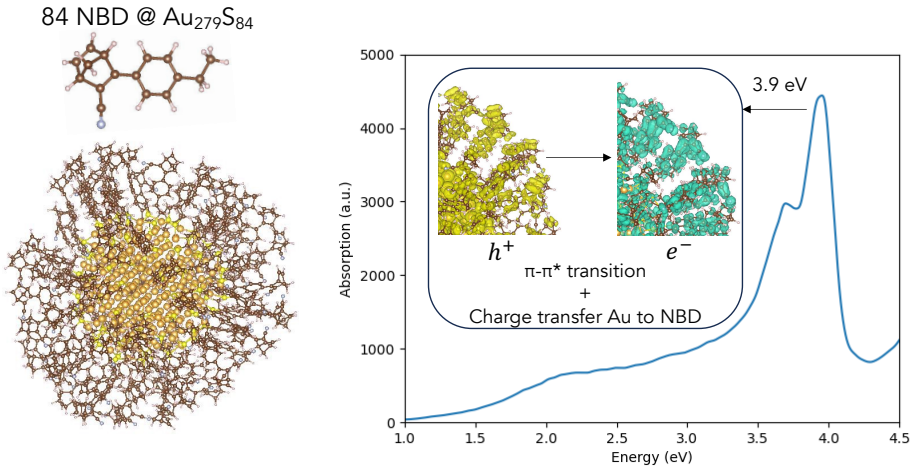

***Figure**: Left: Nanoparticle under study functionalized with photochromes. Right: Computed UV-Visible spectrum and charge density difference under excitation.*

References

- [1] *Chem. Soc. Rev,* **2018**, *47,* 7339-7368.
- [2] *Nat. Chem,* **2014**, *6,* 441-447.
- [3] *J. Chem. Phys*, **2023**, *158(7):*074303.

Flexible and Efficient Semi-Empirical DFTB methods for Electronic Structure Prediction of 3D, 2D Perovskites and Heterostructures

J. Jiang[1], T. van der Heide[2], S. Thébaud[1], C. R. Lien-Medrano[2], M. Zacharias[1], B. Aradi[2], C. Katan[3], T. Frauenheim[4,5,6], J. Even[1]

[1]Univ Rennes, INSA Rennes, CNRS, Institut FOTON - UMR 6082, F-35000 Rennes, France
[2]Bremen Center for Computational Materials Science, University of Bremen, 28359 Bremen, Germany
[3]Univ Rennes, ENSCR, CNRS, ISCR – UMR 6226, F-35000 Rennes, France
[4]School of Science, Constructor University, Bremen 28759, Germany
[5]Beijing Computational Science Research Center (CSRC), 100193 Beijing, China
[6]Shenzhen JL Computational Science and Applied Research Institute (CSAR), 518110 Shenzhen, China

Halide perovskites have garnered significant attention due to their unique properties and potential applications in optoelectronics and energy-related fields. However, the reduction in crystal dimension of perovskite from 3D to low dimensional structures introduces challenges, particularly regarding quantum and dielectric confinements, resulting in larger band gaps and exciton-binding energies. The low dimensional structures imply intrinsically bigger unit cells which makes challenging the application of standard density functional theory (DFT) calculation in terms of computational cost. Furthermore, DFT tends to significantly underestimate band gaps, which is extremely problematic for optoelectronic materials. Density Functional Tight-Binding (DFTB) is a flexible, semi-empirical method based on DFT which capable of simulating large system sizes and offers the possibility of accurate band gap prediction with low computational cost.

In this work, we highlight the application of DFTB methodology for studying the electronic structure, effective masses, and charge density localization in low-dimensional perovskite materials. By employing empirical fitting and parameterization, the DFTB method captures the electronic band structures of model 2D perovskites (e.g., Cs_2PbI_4, BA_2PbI_4, and PEA_2PbI_4). We show good agreement between DFTB results and experimental electronic band gaps, as well as reduced effective masses. This first attempt is promising for further applications to other low-dimensional (1D, 0D, hollow) perovskite nanostructures or 2D/3D perovskite heterostructures with large sizes and complexity, which demonstrated excellent operational stability in solar cell architectures.

Acknowledgements:
The work at institute FOTON acknowledges funding from the M-ERA.NET project PHANTASTIC (R.8003.22), and the European Union's Horizon 2020 program, through an Innovation Action under Grant Agreement No. 861985 (PeroCUBE) and through a FET Open research and innovation action under the Grant Agreement No. 899141 (PoLLoC). J.E. acknowledges financial support from the Institut Universitaire de France.

Nanoarchitectonics of Cluster-Based Building Blocks Applied to the Engineering of Photoelectrodes for Solar Energy Conversion

Adèle RENAUD,[1*] Tatiana LAPPI,[1,2] Yakov GAYFULIN,[2] Nikolai NAUMOV,[2] Soraya Ababou-Girard,[3] Tetsuo UCHOKOSHI,[4,5] Fabien GRASSET,[1,4] Stéphane CORDIER[1]

[1]*Univ Rennes, CNRS, ISCR – UMR 6226, F-35000 Rennes, France*
[2]*Nikolaev Institute of Inorganic Chemistry SB RAS, 630090 Novosibirsk, Russian Federation*
[3]*Univ Rennes, CNRS, IPR-UMR 6251, F-35000 Rennes, France*
[4]*CNRS–Saint-Gobain–NIMS, IRL 3629, LINK, NIMS, 1-1 Namiki, 305-0044 Tsukuba, Japan*
[5]*Research Center for Functional Materials, NIMS, 1-1 Namiki, Tsukuba, Japan*

*adele.renaud@univ-rennes.fr

***Abstract* — Ambipolar materials are a class of compounds that can intrinsically transport and transfer simultaneously both charge carriers, holes and electrons in a comparable way.[1] Unlike conventional unipolar semiconductors in which a type of charge carrier is predominant, ambipolar materials can display p-type and n-type characteristics within a single device, which makes them attractive materials for many different application fields such as sunlight conversion.[2,3] Only few materials such as semiconducting polymers, carbon nanotubes, 2D materials or organic-inorganic hybrid perovskites exhibit ambipolar behaviors.[1,3] Their intriguing intrinsic physical properties result from their specific electronic structures which are not only related to the chemical compositions but also to morphology and size effects.[1,3]**

Recently, the authors have completed this family of materials by a new series of compounds, namely the transition metal cluster (MC) compounds based on Mo_6, Re_6, and mixed $(Mo,Re)_6$ clusters.[4,5] $[\{M_6(Q,X)^i_8\}L^a_6]$ (M = Mo or Re, Q = S ou Se, X = I and L = Cl, I or H_2O) cluster building blocks have a nanosize scale restriction giving them fascinating optical and electronic properties such as molecule-like energy gaps, strong absorption in the visible and/or NIR spectral regions, deep red luminescence or high (photo)catalytic effectiveness.[4-9] They are particularly well suited for nanoarchitectonics[8-10] whose the concept is based on the assembly of nanoscale units to reach new original physical properties.

The concept of nanoarchitectonics applied to the design of photoelectrodes built on cluster core building blocks will thus be presented in this communication. MC-based nanoarchitectonic layers and heterostructures were prepared by electrophoretic deposition process. The control of their composition and design led to the development of new ambipolar photoelectrodes with tailored optoelectronic properties. Beyond the deposition route, the origin and the engineering of the photoconductivity properties of MC-based layers will be discussed before to consider their interest as new light-harvesting layer for the solar energy conversion.

REFERENCES

[1] Y. Ren *et al.*, *RSC*, 1-13, 2020.
[2] S. Z. Bisri *et al*, *Adv. Mater.*, 26, 1176-1199, 2014.
[3] G. Giorgi *et al.*, *J. Mater. Chem. A*, 3, 8981-8991, 2015.
[4] A. Renaud *et al.*, *ACS Appl. Mater. Interfaces*, 14, 1347-1354, 2022.
[5] T. Lappi et al., *Sol. RRL, 2201037, 2023.*
[6] A. Renaud *et al.*, *Electrochimica Acta*, 317, 737-745, 2019.
[7] Y. Zhao *et al.*, *Adv. Energy Mater*, 3, 1143-1148, 2013.
[8] M. Feliz et al., *ChemSusChem*, 9, 1963-1971, 2016.
[9] N. T. K. Nguyen *et al.*, *Sci. Technol. Adv. Mater.*, *23*, 547–578, 2022.
[10] K. Ariga, *Nanoscale Horiz, 6*, 364−378, 2021.

Thermal Management

Thermography in semitransparent media with thermotransmittance

Coline BOURGES[1,2], Stéphane CHEVALIER[1,2], Jérémie MAIRE[1,2*], Alain SOMMIER[1,2], Christophe PRADERE[3] and Stefan DILHAIRE[4]

[1] *Univ. Bordeaux, CNRS, Bordeaux INP, I2M, UMR 5295, F-33400, Talence, France*

[2] *ENSAM, CNRS, Bordeaux INP, I2M, UMR 5295, F-33400 Talence, France*

[3] *EPSYL-ALCEN, F-33400 Talence, France*

[4] *Université de Bordeaux, LOMA, CNRS UMR 5798, F-33400 Talence, France*

*jeremie.maire@u-bordeaux.fr

***Abstract*—We use the temperature dependence of the transmittance in the infrared spectral range to obtain the thermal diffusivity and thermal field in semitransparent materials. We combined our measurements with a Lorentz oscillators model to to highlight the importance of the wavelength choice in measuring the thermotransmittance signal.**

I. Introduction

The measurement of temperature fields is a major challenge for the characterization of energy systems, the development of new materials and the study of chemical or biological reactions.

Infrared thermography [1, 2, 3, 4] is the most widely used method for characterising opaque, non-reflecting media. When this method is applied to semi-transparent media, the latter absorb, reflect and transmit the radiation emitted by their surroundings. Discriminating the signal coming from the sample from stray radiation is therefore a real scientific challenge for these materials. Furthermore, identifying the exact origin of the infrared radiation in the case of a thick sample may not be straightforward.

To overcome this constraint, we have developed a measurement method based on the thermal dependence of the refractive index of materials [5]. Thermoreflectance [6, 7, 8] uses this property to characterize opaque and reflective materials. By analogy, thermotransmittance is the study of the variation of optical transmission as a function of temperature and is particularly adapted to investigate semitransparent materials. This contribution details the methods used to implement thermotransmittance and the results obtained on a glass sample. We also introduce a semi-empirical Lorentz oscillators model to explain our spectroscopic findings.

II. Methods and Results

The thermotransmittance setup used in this work is shown in Fig. 1 alongside the working principle of the measurement. In order to adapt the heating system to the microscopic dimensions required to investigate thermal gradients within short distances, a gold resistive wire has been deposited on the sample. The resistor is powered by an intensity-modulated current that heats the sample by the Joule effect at a low frequency. An infrared camera is then used to measure the signal from the sample at a higher sampling rate. To discriminate between the components of this signal coming from the environment, the proper emission and the transmission of the incoming infrared beam, the camera is synchronized to a chopper and acquires one image when the chopper is close, and one when it is open. Subtracting two such subsequent images enables us to isolate the contribution from the light transmitted through the sample. A Fourier transform is then performed on the resulting set of images to isolate the frequency component corresponding the temperature modulation of the sample.

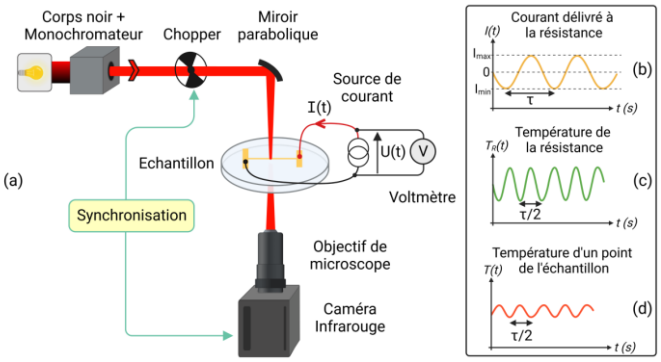

FIGURE 1. Thermotransmittance setup and principle

The phase of the measured signal is used to obtained the thermal diffusivity, which is then used in our thermal model alongside the temperature of the gold resistance measured by the 3ω technique to reconstruct the temperature field in the sample shown in Fig 2. A comparison between this thermal field and the thermotransmittance signal measured then yields the thermotransmittance coefficient.

This procedure is then repeated at different wavelengths, from 3100 nm to 4600 nm, to obtain the thermotransmittance coefficient spectrum of the Borofloat glass sample. To explain our findings, we propose a temperature dependent Lorentz

oscillators model. The results are in good agreement with the measured thermotransmittance values over the spectral range investigated in this study.

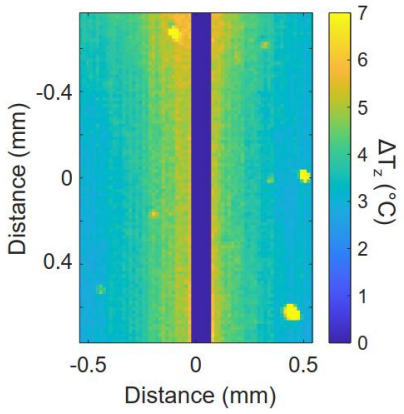

FIGURE 2. FIELD OF TEMPERATURE VARIATION OBTAINED WITH THE THERMOTRANSMITTANCE TECHNIQUE

III. CONCLUSION

In this work we have demonstrated the possibility to use the variation of transmittance with temperature to measure the thermal and thermo-optical properties of semitransparent media. This technique also allows us to obtain the temperature field. In addition, we have developed an optical model based on Lorentz oscillators to explain and predict the origin of the temperature dependence of transmittance in dielectric materials. Our spectroscopic measurements in the range from 3100 to 4600 nm highlight the importance of the wavelength selection in the acquisition of a thermotransmittance signal, with as much as a factor of four in the measured signal between different wavelength in the range of our study.

ACKNOWLEDGMENT

This work was supported by the French National Research Agency (ANR) (Grant ANR-22-CE50-0015).

REFERENCES

[1] G.M. Carlomagno and G. Cardone. “Infrared thermography for convective heat transfer measurements”, *Exp Fluids* 49. 2010.

[2] X. Maldague and S. Marinetti. “Pulse phase infrared thermography,” *Journal of Applied Physics* 79(5) :2694–2698, 1996.

[3] F. Cernuschi, A. Russo, L. Lorenzoni, and A. Figari. “In-plane thermal diffusivity evaluation by infrared thermography,” *Review of Scientific Instruments* 72(10) :3988–3995, 2001.

[4] R. Usamentiaga, P. Venegas, J. Guerediaga, L. Vega, J. Molleda, and F. G. Bulnes. “Infrared thermography for temperature measurement and non-destructive testing,” *Sensors* 14(7) :12305–12348, 2014.

[5] H. H. Li. “Refractive index of silicon and germanium and its wavelength and temperature derivatives,” *Journal of Physical and Chemical Reference Data* 9(3) :561–658, 1980.

[6] David G Cahill. “Analysis of heat flow in layered structures for time-domain thermoreflectance,” *Review of Scientific Instruments* 75(12) :5119–5122, 2004.

[7] S. Dilhaire, S. Grauby, and W. Claeys. “Calibration procedure for temperature measurements by thermoreflectance under high magnification conditions,” *Applied Physics Letters* 84(5) :822–824, 2004.

[8] J. Christofferson and A. Shakouri. “Thermoreflectance based thermal microscope,” *Review of Scientific Instruments* 76(2) :024903–1–024903–6, 2005.

POSTERS

Electronic transport in perovskite

Baker SHALAK, Simon THEBAUD, Jacky EVEN

Institute FOTON, INSA Rennes

3D halide perovskites are gaining attention in the field of solar cell technology due to their remarkable advantages. They excel in converting sunlight into electricity with high efficiency. These materials are cost-effective to produce and can be easily incorporated into various manufacturing processes, making them economically attractive. Their ability to absorb a wide spectrum of sunlight wavelengths enhances their performance, and they hold promise for tandem solar cell setups. However, they do come with challenges. They tend to degrade in humid conditions, raising concerns about long-term stability. Additionally, the presence of lead and sensitivity to temperature variation pose durability issues. Furthermore, exposure to moisture and UV radiation can reduce their performance over time. Therefore, the interest in 2D perovskites in the solar cell field has grown considerably. These materials offer enhanced stability, reduced toxicity, and customizable bandgaps, making them a promising avenue for research and development in solar cell technology. It is important to simulate how electrons move within these materials. Computational techniques based on tight binding and Non-Equilibrium Green's Function (NEGF) simulations are very good tools for understanding the charge carrier's behaviour, predicting and optimizing device performance. These simulations will help us tackle the challenges and maximize the benefits of perovskite materials for sustainable energy solutions.

Molecular dynamics insight of transport properties of mixtures of phase-change materials

Nataliia Kyrychenko[1,2], Liudmyla Klochko[3], Christel Metivier[2], Vasylyi Kuryliuk[1], David Lacroix[2], and Mykola Isaiev[2]

[1]*Faculty of Physics, Taras Shevchenko National University of Kyiv, 64 Volodymyrska Street, Kyiv 01601, Ukraine*
[2]*Université de Lorraine, CNRS, LEMTA, 54000 Nancy, France*
[3]*Université de Lorraine, CNRS, Inria, LORIA, 54000 Nancy, France*

Phase change materials (PCMs) are promising for their application in various systems for thermal energy storage as well as heat management in devices. Thus, improvement of the efficiency of PCMs-based systems can strongly contribute to the development of new pathways for green energy transition. Tackling this issue needs a solid ground based on a better knowledge of the microscopic mechanisms governing transport properties of PCMs.

Molecular dynamics (MD) simulations are efficient tools to obtain atomistic insight about transport properties in small systems. Specifically, the MD has been successfully applied for the evaluation of various rheological and thermal properties such as thermal conductivity, viscosity, diffusion coefficient and heat capacities of pure PCMs [1]. Furthermore, it is important to note that the results of simulations, in this case, are well corelated with experimental ones.

However, from practical point of view, the use of highly pure PCMs in thermal storage devices is often difficult or not realistic. Thus, in the current work we propose to investigate transport properties of mixtures of several PCMs. We will consider several n-alkanes in our simulations as such systems open interesting perspectives for the correlation with experimental results. In this poster, we will present the results of simulations of thermal, mass and momentum transport properties of PCMs composites with various compositions. The temperature dependence of the parameters describing of these properties will be also analyzed.

[1] L. Klochko, J. Noel, N.R. Sgreva, S. Leclerc, C. Métivier, D. Lacroix, M. Isaiev, Thermophysical properties of n-hexadecane: Combined molecular dynamics and experimental investigations,
International Communications in Heat and Mass Transfer, Vol. 137, 2022, 106234

NV Centers in nanodiamonds as a CL temperature probe

Pablo SÁENZ DE SANTA MARÍA MODROÑO[1**] and Gwenolé JACOPIN[1,*]

[1] Institut Néel CNRS/UGA, 25 rue des Martyrs 38042 Grenoble cedex 9

* gwenole.jacopin@neel.cnrs.fr

** pablo.saenz-de-santa-maria-modrono@neel.cnrs.fr

***Abstract*— We have studied the temperature dependence on the CL spectrum of Nitrogen doped nanodiamonds. The results point to a potential nanothermometry probe with high spatial resolution**

I. INTRODUCTION

As electronic devices become smaller, measuring their core properties with an adequate spatial resolution becomes increasingly more challenging. Particularly, the electrical resistance of a small channel can be greatly enhanced due to local defects. These defects create "hot spots" due to joule heating during operation [1]. Measuring temperature value and gradient in real time with a high spatial resolution would allow for much better characterization of device performance.

However, most developments in luminescence based thermometry focus on photoluminescence (PL) thermometry [2]. This particular technique is based on the PL spectrum of fluorescent nanoparticles and its relation with temperature. Interest in this technique stems from biology, since by being fully optical, it does not cause tissue damage. Concerning semiconductor studies, the main advantage of luminescence based thermometry is to monitor the local temperature without the need of electrical contact.

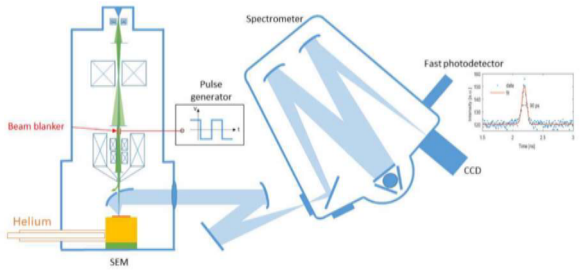

FIGURE 1 – EXPERIMENTAL SETUP.

The main drawback of PL thermometry for nanodevice characterization is the low spatial resolution, unavoidable due to the diffraction limit of light [3]. To improve the spatial resolution, we propose developing a similar technique: cathodoluminescence-based nanothermometry. As the name suggest, the methodology is similar to that of PL nanothermometry, but using nanoparticles whose cathodoluminescence (CL) spectrum is temperature dependent. This would enhance the resolution to that of CL, allowing for much more spatially precise temperature imaging.

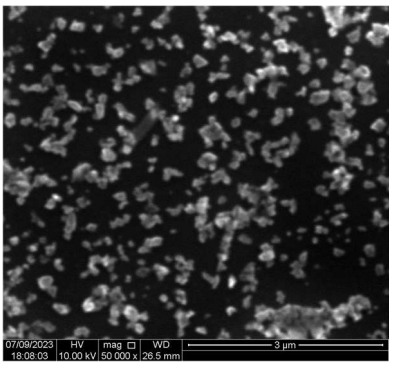

FIGURE 2 – NANODIAMONES SPREAD OVER A SI SUBSTRATE

Figure 1 shows the specificity of the setup used. The electrons were produced in a SEM model FEI Inspect F50, which allows to simultaneously perform CL and imaging. The spatial resolution is 50 nm. The SEM is equipped with a Janis helium cryostage, which allows for a temperature range between 5 and 300 Kelvin.

The CL spectra was collected using a parabolic mirror, and introduced into a spectrometer with a grating of either 600 or 1800 g/mm. The spectrometer signal was sent to either a fast photodetector, which allows for quick spatial mappings of the chosen wavelength; or to a CCD which can measure the CL spectrum with a maximum spectral resolution of 0.1 nm.

II. EXPERIMENTAL RESULTS

To develop CL nanothermometry for nanocircuits, we need a CL reactive nanoparticle that can resist the potentially high energy of both the SEM electrons and the carriers from the studied sample. We want a particle that wont chemically react with the sample, that is stable over a large range of temperatures, and that whose CL spectra is both as bright as possible, and

sensitive to temperature. Diamonds with Nitrogen Vacancy (NV) centers fulfill all those requirements.

The NV center in diamonds is a defect caused by the substitution of a carbon atom by a Nitrogen one and the removal of one of its first neighbors [5]. The defects break lattice symmetry, causing the localization of carriers and the *de facto* behavior of an embedded molecule. These types of defects can be negatively charged or neutrally charged [6]. Most studies have focused on the properties of the negatively charged center, due to its quantum behavior. However, we focused on the properties of the neutrally charged NV centers.

Neutrally charged NV centers have a Cathodoluminescence emission peak at a wavelength of 575 nm [4]. The peak's intensity and shape are strongly dependent on temperature, turning it into a promising candidate for developing CL nanothermometry. The dependence of the peak is particularly strong above 100 Kelvin.

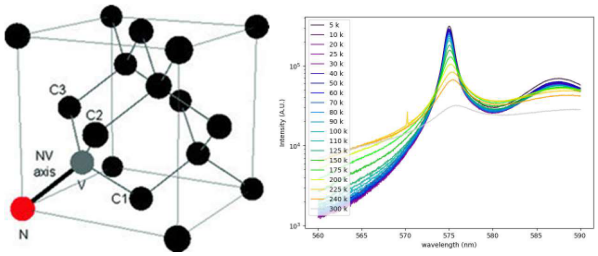

FIGURE 3 - (LEFT) STRUCTURE OF THE NV CENTER IN DIAMOND. RIGHT. (RIGHT) CL SPECTRA OF THE NV^0 LUMINESCENCE AS A FUNCTION OF THE TEMPERATURE.

We have also observed a second peak at 389 nm at low temperature, shown in figure 4. This peak origin is currently unknown [7], but our results point strongly in the direction of a nitrogen effect, since it only present in nanodiamonds with neutrally charged NV centers. This peak has a much lower brightness, but doesn't disappear at higher temperatures, and its shape is also temperature dependent.

We have spread commercial Nitrogen-doped nanodiamonds on top of a Silicon wafer, as seen in figure 2. By using a helium based cryostat, we measured the spectra of the samples at different tabulated temperatures. The change in intensity and full with at half maximum on the 575 nm peak was quite drastic, as we can see in figure 3.

Since the intensity of the peak is highly dependent on the measurement conditions, we choose the full with at half maximum (FWHM) and the temperature-dependent parameter. Results can be seen in figure 4. Its behavior is very consistent between nanodiamonds, but its absolute value changes between the individual samples. This means that the may better suited as relative temperature sensors.

The nanodiamonds have an average size of a 100nm, and can form a thin layer when spread on top of a sample. By using electrons with a low acceleration voltage (3 KeV) we can prevent the beam from entering the material bellow the diamond. This ensures that the CL signal studied comes entirely from the nanodiamonds, eliminating a potential source of noise. Even with this low energy, CL intensity was extremely high, as is common in diamond samples, which allows for high accuracy even with low exposure times.

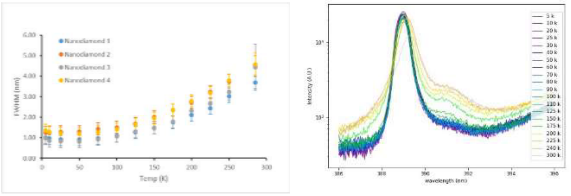

FIGURE 4 – (LEFT) FULL WIDTH AT HALF MAXIMUM OF NV PEAK FOR MULTIPLE INDIVIDUAL NANODIAMOND. (RIGHT) NITROGEN-REALTED PEAK AT 389 NM.

III. CONCLUSIONS AND PERSPECTIVE

The change with temperature of the FWHM NV peak is very consistent between nanodiamonds, but its absolute value changes between the individual samples. This means that the may better suited as relative temperature sensors. Further measurements will be performed on highly dense nanodiamond coating to see if this variation is also present.

The error associated to the FWHM also grows at higher temperatures due to the peak vanishing at 300 Kelvin. The 389 nm peak may be a potentially preferable sensor at those values.

ACKNOWLEDGMENT

This work was supported by the French National Research Agency (INDIANA Project No. ANR-21-CE42-0020-01).

REFERENCES

[1] Avram Bar-Cohen and Peng Wang. "On-chip Hot Spot Remediation with Miniaturized Thermoelectric Coolers". In: *Microgravity Science and Technology* 21.1 (Aug. 2009), pp. 351–359.

[1] Jaque, Daniel & Vetrone, Fiorenzo. (2012). "Luminescence nanothermometry". *Nanoscale*. 4. 4301-26. 10.1039/c2nr30764b.

[3] Abbe, E. Beiträge "zur Theorie des Mikroskops und der mikroskopischen Wahrnehmung." *Archiv f. mikrosk. Anatomie* **9**, 413–468 (1873).

[4] Manson, N. B. et al. "Assignment of the NV0 575 nm zero-phonon line in diamond to a 2E-2A2 transition". *Physical Review* B 87, 155209. issn: 1098-0121, 1550-235X. arXiv: 1301.3542 (Apr. 25, 2013)

[5] Jensen, K., Kehayias, P. & Budker, D. "Magnetometry with Nitrogen-Vacancy Centers in Diamond" 553–576. isbn: 978-3-319-34068-5 (Sept. 1, 201)

[6] Manson, N. B. et al. "NV- N+ pair centre in 1b diamond". *New Journal of Physics* 20, 113037. issn: 1367-2630 (Nov. 2018)

[7] Zaitsev, A. M. "Optical Properties of Diamond" isbn: 978-3-662-04548-0 (Springer Berlin Heidelberg, Berlin, Heidelberg, 2001)

Optical Properties of Ni-Porphyrin Encapsulation in Carbon Nanotubes for Organic Nano-Hybrid Solar Cells: A DFT Study

Anass EL FATIMY[1,2], Mourad BOUTAHIR[1,*] ,Abdelali RAHMANI[1], and Konstantinos TERMENTZIDIS[2]

[1] *Laboratoire d'Etude des Matériaux Avancés et Applications (LEM2A), Université Moulay Ismail,FSM-ESTM, BP 11201, Zitoune, 50000 Meknes, Morocco*

[2] *Laboratoire CETHIL UMR 5008, CNRS, INSA of Lyon, Un. Claude-Bernard Lyon 1, INSA de LYON 9 Rue de la Physique 69100, FRANCE*

*corresponding author: anass.el-fatimy@insa-lyon.fr

***Abstract*— In this study, we explore the feasibility of integrating Nickel porphyrin molecules into a semiconducting single-walled carbon nanotube, thereby forming an active layer for solar cell devices. Using density functional theory, we investigated the optoelectronic characteristics of the isolated Nickel porphyrin molecule and two distinct configurations of the hybrid system. Our investigation highlights that the structural stability can be attributed to the exchange of electrical charge between the Nickel porphyrin molecules and the nanotube. Specifically, Nickel atoms were deliberately selected due to their notable influence on the electronic properties of the hybrid systems, resulting in increased light absorption, enhanced charge separation, and greater power conversion efficiency in solar cell devices. These findings imply that encapsulated systems featuring type II heterojunctions hold significant potential as effective charge carriers and light absorbers within the active layer of organic solar cells that rely on filled single-walled carbon nanotubes. This research could contribute significantly to the advancement of highly efficient organic solar cells utilizing filled semiconducting single-walled carbon nanotubes.**

I. INTRODUCTION

The topic of increasing energy consumption and the imperative to transition away from fossil fuels has been a subject of ongoing discussion renewable energy sources are widely acknowledged as a sustainable, long-term solution to replace conventional fuels. Within this realm, solar energy stands out as a particularly vital focus of research in optoelectronic devices due to its abundance and potential[1]. Solar cells, in particular, possess the ability to capture sunlight and convert it efficiently into electrical energy. In recent years, there has been a growing interest in organic solar cells (OSCs) that employ π-conjugated materials*., driven by advancements in materials and manufacturing processes. Currently, the dominant technology for photovoltaic systems relies on silicon cells with a band gap[2] of 1.2 eV. However, the substantial costs associated with their production and installation present a barrier to these systems competing effectively on a global scale with fossil fuels, primarily due to their high expense[3]. Hence, by enclosing conjugated molecules within single-walled carbon nanotubes (SWCNTs), it becomes feasible to safeguard them from degradation. In general, this method is widely acknowledged as one of the most effective techniques for integrating the physical characteristics of two systems without causing any mechanical or chemical harm to either of them[4]. The benefits provided by these encapsulated nanohybrid systems render them highly suitable for commercial applications. In this research, the primary aim was to investigate the optical properties of SWCNT loaded with Nickel-porphyrin molecule, which resulted in significant improvements in both the electrical and optical properties of the SWCNTs[5]. SWNTs possess the unique ability to accept electrons and act as electron donors while absorbing light. They represent the most complex one-dimensional (1D) materials, resembling cylindrical structures constructed from a conjugated sp^2 carbon lattice, characterized by smooth and impermeable walls. This paper delves into the optical characteristics of the key components used in organic solar cells, with a specific focus on a type of metallo-porphyrins containing a single Nickel atom (NiP). Our primary emphasis was on analyzing the optical properties of an individual strand of the NiP molecule when it is confined within a SWCNT.

II. MODEL AND METHODOLOGY

We employed first-principles calculations, which are grounded in density functional theory (DFT) and supported by prior research[6] to assess the properties of NiP molecule when it's confined within SWCNT. For the analysis of hybrid system, we applied the Vienna ab initio Simulation Package (VASP)[7], utilizing a plane-wave basis set with projector-augmented waves. Our methodology involved the use of DFT calculations with the generalized gradient approximation (GGA).

We utilized noncovalent functionalization to create a model system that involves enclosing NiP molecule within an SWCNT. We investigated this system in two different molecule orientations, as depicted in Figure 1. In the setups referred to as NiP@SWCNT, the molecule's frontal plane is oriented vertically relative to the nanotube's axis. On the other hand, in the configurations designated as NiP*@SWCNT, the molecule's horizontal plane is aligned parallel to the nanotube's axis.

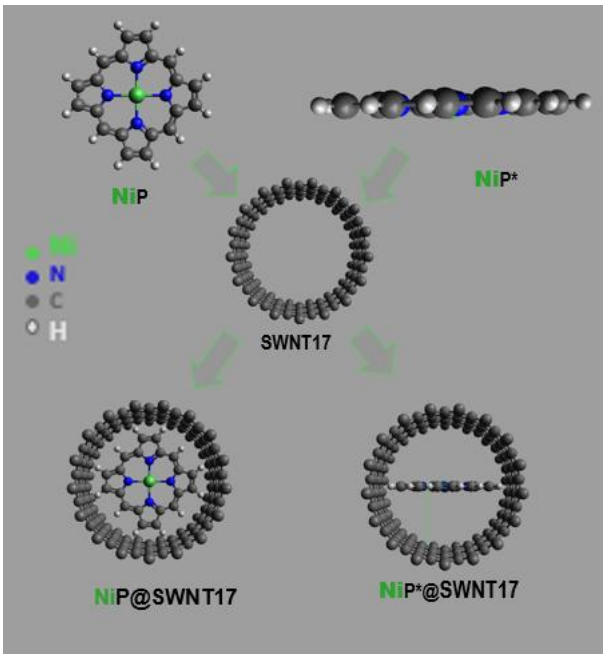

Figur 1. Structure Overview: Encapsulation of Porphyrin Systems NiP@SWNT17 and NiP*@SWNT17

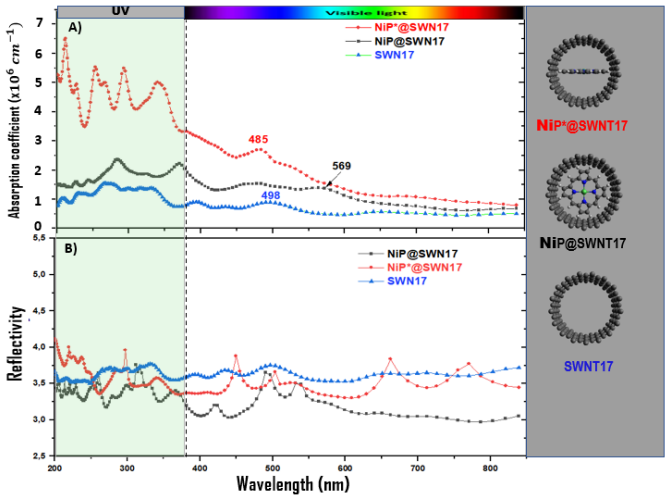

Figure 2. Analysis of Optical Properties for Pristine SWNT17, NiP@SWNT17, and NiP*@SWNT17 Using GGA Functional: (A) Spectral Absorption Coefficient. (B) Reflectivity Spectrum

III. Results and Conclusion

In this research, the optical characteristics of nano-systems encapsulating certain materials were analyzed within the DFT framework. The optical properties of hybrid structures comprising Single-Walled Carbon Nanotubes and Nickel-porphyrins are notably influenced by the inclusion of Nickel atom. These hybrid structures exhibit pronounced optical absorption in both the visible light and UV regions. In comparison to isolated SWCNTs, the hybrid structures containing a Ni atom show a slight shift in their absorption edges towards higher energy levels. As for reflectance, the hybrid structures generally display lower reflectance intensities when compared to isolated SWCNTs, indicating improved light-capturing capabilities. This suggests an enhanced capacity for light absorption and the potential for efficient energy conversion. The significance of these hybrid structures in solar cell devices is quite remarkable. Their robust absorption of visible light and effective separation of charges between the metalloporphyrin and SWCNT components facilitate functional charge separation, a crucial element for augmenting the power conversion efficiency (PCE) of organic solar cells (OSCs). These hybrid systems exhibit a type II bulk heterojunction configuration, which enables efficient separation of photogenerated charge carriers. This characteristic is highly desirable for promoting efficient charge transport and enhancing the PCE in OSCs.

Acknowledgment

The work was supported by Moulay Ismail University Research Support (13-16), Laboratoire CETHIL in INSA of LYON, GOUVERNEMENT FRANCAISE and Comisión Nacional de Investigación Científica y Tecnológica (CONICYT)-Fondo Nacional de Desarrollo Científico y Tecnológico (FONDECYT) Posdoctodado 2020 Nº 3200046. JML acknowledges support from Financiamiento basal para centros científicos y tecnológicos de excelencia AFB180001.

References

[1] Wang, Dian and Wright, Matthew and Elumalai, Naveen Kumar and Uddin, Ashraf, "Stability of perovskite solar cells", Solar Energy Materials and Solar Cells, 147. 255—275 ,2016.

[2] Green, Martin A," The path to 25% silicon solar cell efficiency: History of silicon cell evolution.", Progress in photovoltaics, 17. 183—189, 2009.

[3] Polman, Albert and Knight, Mark and Garnett, Erik C and Ehrler, Bruno and Sinke, Wim C," Photovoltaic materials: Present efficiencies and future challenges", Science, 352. 6283. 44-24, 2016.

[4] Dinadayalane, TC and Gorb, Leonid and Simeon, Tomekia and Dodziuk, Helena," Cumulative $\pi - \pi$ interaction triggers unusually high stabilization of linear hydrocarbons inside the single-walled carbon nanotube", International Journal of Quantum Chemistry, 107. 12. 2204-2210, 2007.

[5] Boutahir, Mourad and Chenouf, Jamal and Mejïa-Lopez, Jos{\'e} and Rahmani," Role of carbon nanotubes as an acceptor to enhance the photovoltaic performances of organic solar cells based on π-conjugated thiophene as a donor materials", International Journal of Energy Research, 45 .11.16242—16253, 2021.

[6] Eichkorn, Karin and Treutler, Oliver and Ohm, Holger and Haser, Marco and Ahlrichs, Reinhart, "Auxiliary basis sets to approximate Coulomb potentials", Chemical physics letters, 240. 4. 283—290, 1995.

[7] Kresse, Georg and Furthmu}ller, Jurgen, "Efficient iterative schemes for ab initio total-energy calculations using a plane-wave basis set", Physical review B, 54. 16 .11169 ,1996.

Perforated Graphene for Thermal Rectification

Markos POULOS[1,*] and Konstantinos TERMENTZIDIS[2]

[1] *University of Lyon, INSA de Lyon, CETHIL UMR5008, Villeurbanne, 69100, FRANCE*

[2] *University of Lyon, CNRS, INSA de Lyon, CETHIL UMR5008, Villeurbanne, 69100, FRANCE*

*markos.poulos@insa-lyon.fr

***Abstract*—Non-Equilibrium Molecular Dynamics simulations were performed to study thermal rectification effects in perforated graphene monolayers with various geometrical pore parameters. Circular and triangular pores have been used. The Thermal Rectification (TR) ratios found are of the order of 6.5%. Phonon overlap mismatch and directional scattering have been proposed as possible mechanisms of thermal rectification in these systems.**

I. INTRODUCTION

Continuous miniaturization of devices leads to hotspots that limit their efficiency; we thus need efficient heat management strategies at the nanoscale. Still, efficient nanoscale thermal diodes, which can contribute towards this end, are not yet fully developed. Systems studied in the literature for thermal rectification include: TMDC lateral heterostructures [1], hBN-graphene Van der Waals heterostructures [2], trapezoidal and T-shaped graphene nanoribbons [3], thickness asymmetric graphene nanoribbons [4], etc. In this work we studied the thermal rectification performance of asymmetrically perforated graphene monolayers and the impact of perforation in its thermal conductivity.

II. METHODOLOGY

A. Non-Equilibrium Molecular Dynamics (NEMD)

Thermal conductivity in out-of-equilibrium systems is calculated using the NEMD method, where a thermal bias (in this case a temperature gradient ∇T across the length of the system) is applied and after reaching steady-state, the response is measured (in this case the steady-state thermal current I). The thermal conductivity κ is then given by Fourier's expression:

$$\kappa = \left(\frac{I}{A}\right) \cdot \frac{1}{\nabla T} \quad (1)$$

where A is the system's cross section perpendicular to the gradient.

B. Phonon Wavepacket Propagation (PWP)

Propagation of particular phonon modes and their interaction with the characteristic features of the nanostructures can be studied using the PWP, where a mechanical time-dependent force is applied to an excitation region in order to excite a specific phonon wave packet. The force is a Gaussian-windowed plane wave and its time-dependence is given by the expression [5]

$$f(t) = A\sin[2\pi\nu(t-3\tau)] \cdot exp\left[-\frac{(t-3\tau)^2}{(2\tau)^2}\right] \quad (2)$$

where A is the amplitude and τ the spreading of the Gaussian

C. Systems Studied

In this work we studied the impact of nano-perforation in graphene monolayers. In the first part, we studied the impact of the distribution of diameters and neck sizes of circular pores in the thermal conductivity of graphene. In the second part, we studied the thermal rectification effects in perforated/pristine graphene lateral heterostructures, in which the pores were either circular or triangular, and for the last case both orientations of the triangle apexes with respect to the pristine part were studied.

III. RESULTS AND DISCUSSION

A. Impact of Pore Distribution on Thermal Conductivity

As can be seen from Figure 1, even a slight porosity of 12% can dramatically reduce the thermal conductivity of graphene. Also, keeping the porosity constant, we observe that varying the pore diameters along a gradient reduces the conductivity even more; this we attribute to a further restriction of the phonon pathways along the thermal gradient, compared to the other configurations (see Figure 1).

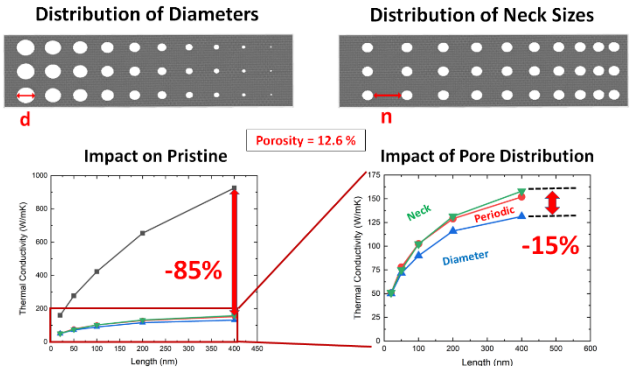

FIGURE 1. EFFECT OF VARIOUS PERFORATION CONFIGURATIONS ON THE THERMAL CONDUCTIVITY OF MONOLAYER GRAPHENE.

B. Rectification: Circular Pores+Pristine

In this second part, we investigated the impact of perforation on the thermal conductivity and thermal rectification effects of a perforated/pristine graphene lateral heterostructure, by keeping the perforated part constant at $l_{perf} = 50\ nm$ and a porosity of 50%, and increasing the length of the pristine side. While the thermal conductivity increases monotonously, the thermal rectification ratio increases to a maximum value of 6% for $l_{pristine} = 250\ nm$ and decreases thereafter. The directionality of the rectification also changes non -monotonously (see Figure 2)

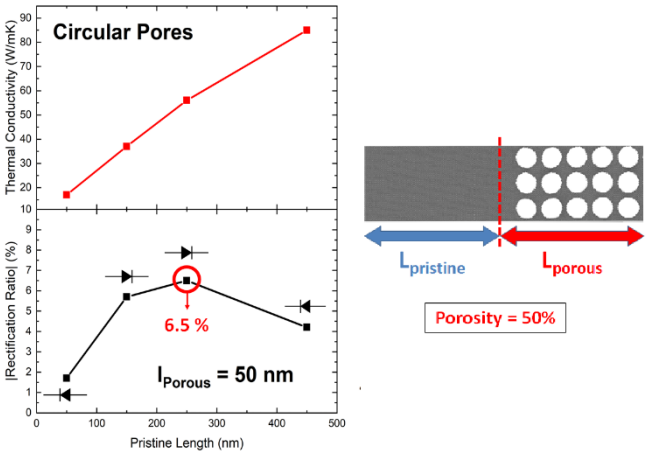

FIGURE 2. IMPACT OF PRISTINE SIDE LENGTH ON THE THERMAL CONDUCTIVITY AND THERMAL RECTIFICATION OF PRISTINE/PERFORATED GRAPHENE HETEROSTRUCTURES: CIRCULAR PORES.

C. Rectification: Triangular Pores+Pristine

Lastly, we repeated the above study in a heterostructure with triangularly-shaped pores and a porosity of 32%, where the pores' apexes were oriented both towards and away from the pristine part (figure 3, right). In this case, the thermal rectification ratios change monotonously (figure 3. left) and their directionality only depends on the orientation of the triangles (figure 3. right).

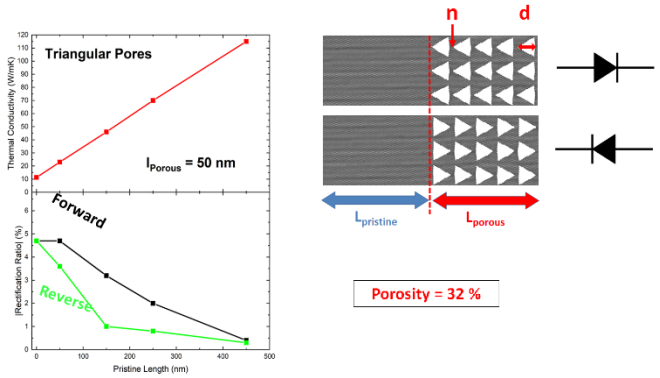

FIGURE 3. IMPACT OF PRISTINE SIDE LENGTH ON THE THERMAL CONDUCTIVITY AND THERMAL RECTIFICATION OF PRISTINE/PERFORATED GRAPHENE HETEROSTRUCTURES: TRIANGULAR PORES.

In order to directly investigate this behavior, we performed PWP simulations for the propagation of ZA phonon with energy $\omega = 200\ cm^{-1}$ in both configurations. As is seen from Figure 4, this behavior can be explained by the enhanced scattering of incident phonons when the apexes are facing away from the source (middle part).

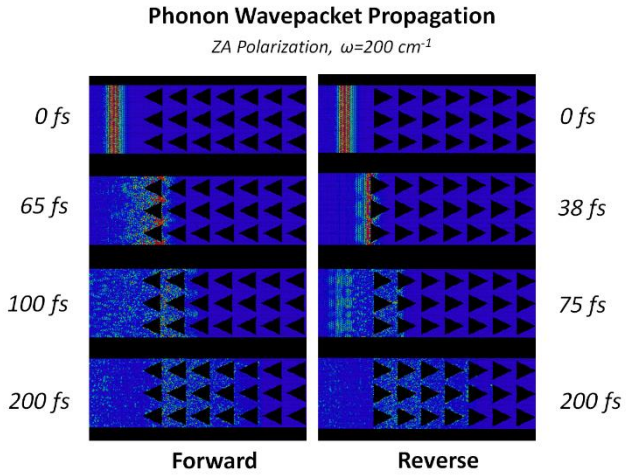

FIGURE 4. PROPAGATION OF A PHONON WAVE-PACKET IN A PERFORATED GRAPHENE MONOLAYER WITH TRIANGULAR PORES. BOTH ORIENTATIONS OF THE PORES WITH RESPECT TO THE SOURCE ARE STUDIED.

IV. CONCLUSIONS

Perforation dramatically lowers the thermal conductivity of pristine graphene, even for small porosities. Thermal rectification can be a result of different mechanisms, such as phonon mode mismatch and directional scattering. Finally, triangular pores with different orientation scatter phonons differently; this is a source of directional scattering that potentially leads to thermal rectification.

REFERENCES

[1] Zhang et al., *Science* **378**, 169-175 (2022)
[2] Chen et al., *ACS Appl. Mater Interfaces* **12**, 15517-15526 (2020)
[3] Wang et al., *Nano Lett.* **378**, 169-175 (2013)
[4] Zhong et al., *Appl. Phys. Lett.* **99**, 193104 (2011)
[5] Desmarchelier et al., *Phys. Rev. B.* **103**, 014202 (2021)

Lorenzo PAULATTO
IMPMC – CNRS UMR7590/Sorbonne Université/MNHN/IRD
4 place Jussieu – 75005 Paris

Phonon thermal conductivity in micron-sized samples

The last ten years have seen a dramatic improvement in theoretical methods to approach lattice-driver thermal conductivity. Starting from reliable algorithms for the exact solution of Boltzman-Peirels transport equation, inclusion 4-phonon scattering term and of incoherent Allen-Feldmann transport mechanism, transport from equilibrium molecular dynamics. These techniques have allowed the exploration of extreme materials and conditions: ultra-low temperature, hydrodynamic regime, large unit cells, proximity structural instabilities. On the other hand, the effect of finite size and lattice defects (vacancies, substitutions, misalignment) while very much present in real samples, is less well studied. One approach is to model the flight time between defect that can be used to associate an effective lifetime to defects and boundaries.
We will present two examples to compare effective and exact modelization of finite size effects: the effect of stacking defects in Bi2Se3 and of finite size Bi2Se3 nanoslabs [1], and the comparison of simplified versus explicit modeling of Silicon nanowires [2].

[1] L. Paulatto, D. Fournier, M. Marangolo, M. Eddrief, P. Atkinson, and M. Calandra, *Thermal Conductivity of Bi2Se3 from Bulk to Thin Films: Theory and Experiment*, Phys. Rev. B **101**, 205419 (2020).
[2] K. R. Hahn, C. Melis, F. Bernardini, L. Paulatto, and L. Colombo, *Thermal Transport in Ultrathin Si Nanowires: A First Principles Study*, arXiv:2207.02082.

Semi-empirical modeling of low-dimensional metal-halide perovskites

Simon Thébaud[a], Tan Nguyen[b], Claudine Katan[b], Jacky Even[a]
[a] Univ Rennes, INSA Rennes, CNRS, Institut FOTON, UMR 6082, Rennes
[b] Univ Rennes, ENSCR, CNRS, ISCR, UMR6226, Rennes

In the last decade, metal-halide perovskites have emerged as superstar materials for optelectronic applications due to their high absorption – comparable to classical III-V semiconductors – and their defect tolerance leading to robust charge transport properties. As photovoltaic absorber materials, in particular, they have already reached the efficiency of silicon for a small fraction of the material requirement and price. To overcome stability issues faced by bulk perovskite compounds, layered perovskite structures are used in which charge carriers are confined in ultrathin quantum wells (a few angstroms to tens of angstroms). Moreover, perovskite nanocrystal quantum dots are promising platforms for other applications such as single-photon and entangled photon emission. In these low-dimensional structures, confinement effects give rise to strong Coulomb interactions between electrons and hole, leading to bound excitons. In this poster, I will present some of our work to model these systems using tight-binding and semi-empirical methods.

Simulation of Hot Carriers Using ab-initio Parameters for Energy Harvesting

Mohamad GHANEM [1], Raja SEN [2], A.Pilotto[1,3], Jelena SJAKSTE [2], and Jerome SAINT-MARTIN [1]

[1] *Université Paris Saclay, Centre de Nanosciences et de Nanotechnologies, 91120, Palaiseau, France*

[2] *Ecole Polytechnique, Rte de Saclay, 91120, Palaiseau, France*

[3] *University of Udine, Palazzo Florio, Udine, Friuli Venezia Giulia, Italy*

Abstract-- In this work, we present the development of Monte Carlo code to study the transient regime of hot carriers in GaAs using a new methodology based on applying DFT band structure and scattering rates inputs.

I. Introduction

Standard solar cells, which are good example of energy harvesting devices, exhibit an efficiency limited by their inability to exploit all the excess energy of photo-induced carriers. A solution for that could be considering specific hot carrier solar cells instead [1]. In this context, a new methodology that studies easily the evolution of hot carriers in 2D materials and wide range semiconductors should be created. Accordingly, a Full Band Monte Carlo code is being developed to read DFT inputs. The code is being tested on a well-known material 'GaAs' before moving to other semiconductors and in particular 2D materials.

II. Method

A. Ab-initio material properties

The electronic band structure was calculated by using an ab initio method in the frame works of DFT and DFPT in Quantum Espresso suite. The considered GaAs lattice constant was $5.53A^0$. The electronic band structure was described using local density approximation (LDA) and a 16x16x16 set of k-points was used. The kinetic-energy cutoff of the plane-wave basis set was fixed at 70 Ryd.

For the carrier-phonon scattering rates, the data being tested.

B. Monte Carlo simulation

To study the evolution of carriers with time, Boltzmann Transport Equation (BTE) is solved using stochastic Monte Carlo code [2] which computes the free flight of carriers and force them to move. After that, a scattering mechanism with a new state is chosen by the help of stochastic probability and a rejection technique. To test DFT scattering rates, we save all scattering rates between two states in the First Brillouin Zone S(k:k') (Fermi Golden rule) and remove the rejection technique. The first saved data was computed using Empirical Pseudo Methods (EPM) in order to test the code's development.

$$S_i(\vec{k},\vec{k'}) = \frac{2\Pi}{\hbar}\left|\langle\vec{k'}|H_i|\vec{k}\rangle\right|^2 \varphi_{k'}\,\delta(E' - E - \hbar w_i)$$

Where:

$\vec{k}$, E are the initial state and energy respectively.

$\vec{k'}$, E' is the final state and energy respectively.

H_i is the electron-phonon interaction Hamiltonian.

$\varphi_{k'}$ is the final state density.

$\hbar w$ is the phonon energy.

III. Results

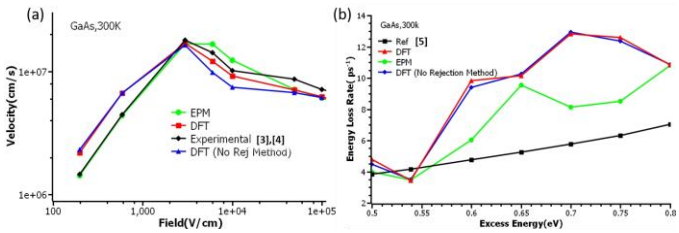

FIGURE 1. (a) Velocity versus different electric field values at stationary regimes. (b) Energy loss rate of particles versus initial excess energies

Curve	Band Structure	Scattering rates	Technique
	EPM	EPM	Rejection method No S(k,k') inputs
	DFT	EPM	Rejection method No S(k,k') inputs
	DFT	EPM	No Rejection method S(k,k') inputs

TABLE 1. Description for the band structure, scattering rates, and technique used for each curve.

In table 1, we represent the type of band structure, scattering rate, and technique used for each curve. We study the velocity versus field curve before and after substituting DFT band structure and also after the code development to be able to read DFT scattering rates. The results are very similar to previous experimental results [3], [4]. In second figure, for energy relaxation, energy loss rate is computed versus excess energies. The difference seen compared to previous simulation results [5] should be fixed after using DFT scattering rates.

IV. Conclusion

We have developed a Monte Carlo code that study the transient regime of hot carriers and is ready to test ab initio calculations. This code could allow us to test transient regime in 2D materials when GaAs test is finalized.

References

[1] S.Kahmann, M.A.Loi, Journals of Materials Chemistry C, Vol 7, 2019

[1] A. Piloto, "MODELING AND OPTIMIZATION OF SINGLE PHOTON AVALANCHE PHOTODIODES FOR X-RAY DETECTION," 2021.

[3] P. A. Houston, A.G.R. Evans, Solid-State Electronics, Vol 20, 1977

[4] W.T.Masselink, N.Braslau, W.I.Wang, Applied Physics Letters, Vol 51, 1987

[5] H.Tanimura, J.Kanasaki, K.Tanimura, Physical Review B, Vol 93, 2016

Applying Machine Learning for the Prediction of Thermal Properties of Materials from the Material Database Project

L. Klochko[a], L. Chaput[a,b] and M. D'Aquin[a]

[a] Université de Lorraine, CNRS, LORIA, France
[b] Institut Universitaire de France, 1 rue Descartes, 75231 Paris, France

With the availability of large, open databases of material descriptions (such as Material Database Project [1]), the use of deep learning techniques is growing, as is the use of machine learning to predict the physical properties of different compounds. These applications are expected to speed up processes such as materials interaction discovery [2] for instance. The ability of deep learning approaches to handle complicated, rich, and raw data—like the crystalline structure of materials—through massive neural networks is a significant advantage over more standard machine learning techniques, which would depend on human chosen and designed features.

In our work, we developed supervised AI model that allow us to predict the lowest thermal conductivity (LTC) with threshold = 14.5 W/m*K) searched over Material Database Project [1]. To train our model, we used data on thermal conductivity, volumes, and densities, as previously computed in [3]. These computations were carried out for materials falling under three different space groups: rocksalt, zincblende, and wurtzite, encompassing a total of 103 different compounds. Our preliminary model training experiments have revealed the promise of employing the Random Forest (RF) algorithm [4]. As a result of the trainings of our model with different selections of the depth of the algorithms, we were able to reach impressive results for Mean Score Test (see Fig.1).

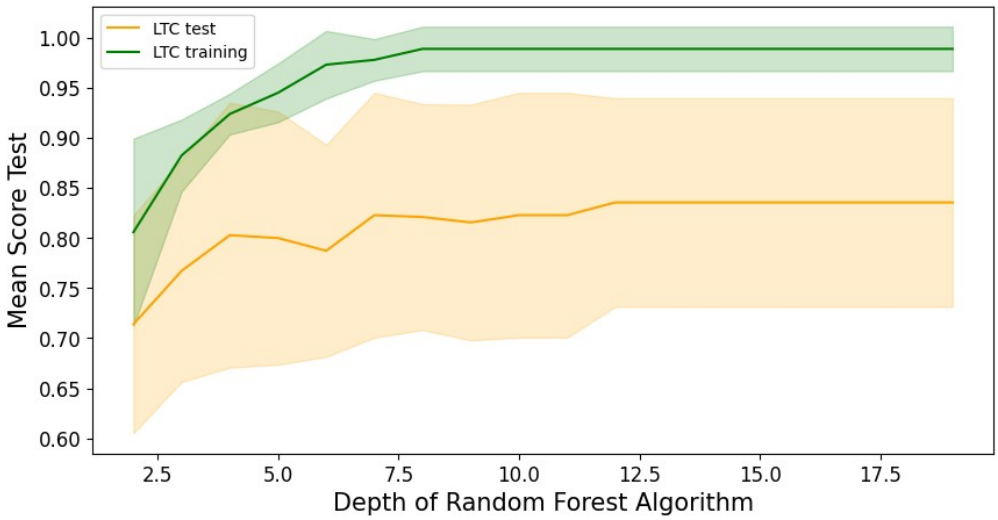

Fig.1: The Mean Score Test results dependence on the depth of RF algorithm for our AI model for predicting the lowest thermal conductivity (threshold = 14.5 W/m*K) (LTC).

References:

[1] A. Jain*, S.P. Ong*, G. Hautier, W. Chen, W.D. Richards, S. Dacek, S. Cholia, D. Gunter, D. Skinner, G. Ceder, K.A. Persson *(*=equal contributions)* *The Materials Project: A materials genome approach to accelerating materials innovation* APL Materials, 2013, 1(1), 011002.

[2] Chen, C., Ong, S.P. A universal graph deep learning interatomic potential for the periodic table. *Nat Comput Sci* **2**, 718–728 (2022).

[3] Seko, A. et al. Prediction of low-thermal-conductivity compounds with first-principles anharmonic lattice-dynamics calculations and Bayesian optimization. Phys. Rev. Lett. 115, 205901 (2015).

[4] Ho, T. K. (1995). Random decision forests. In Proceedings of 3rd international conference on document analysis and recognition (Vol. 1, pp. 278–282).

Influence of domain walls on the thermal conductivity of $ErMnO_3$ ceramics

R. BELRHITI NEJJAR[1,*], F. GIOVANNELLI[1], J. SCHULTHEIß[2], M. HAAS[2], D. MEIER[2], G. F. NATAF[1,**]
[1] *GREMAN UMR7347, CNRS, University of Tours, INSA Centre Val de Loire, 37000 Tours, France*
[2] *NTNU Norwegian University of Science and Technology Høgskoleringen 1, Trondheim 7034, Norway*

*rachid.belrhiti-nejjar@etu.univ-tours.fr
**guillaume.nataf@univ-tours.fr

Manipulating heat flows remains today a challenge. Yet, this control is critical for a better energy management of our home appliances. Recent experimental results show that ferroelectric oxides can be used to obtain a dynamic heat flow control [1,2]. Ferroelectric oxides spontaneously exhibit domains – whose boundaries are called domain walls – where the positions of the atoms are slightly different [3]. These walls have a direct impact on the propagation of phonons conducting heat. The higher the density of domains, and thus the density of domain walls, **the higher the number of phonons-domain walls collisions and the lower the thermal conductivity**. In this work we studied $ErMnO_3$ polycrystalline ceramics, an improper ferroelectric material. These ceramics were cooled down at different rates around the Curie temperature to obtain different sizes of ferroelectric domains. On the one hand, we worked with four ceramics with the same grain size but different domain sizes to highlight the influence of domains. On the other hand, we worked with three ceramics with different grain sizes and different domain sizes because in $ErMnO_3$, when the grain size decreases, the domain size increases [4].

Our results demonstrate that **the size of ferroelectric domains plays an important role in influencing the thermal conductivity of $ErMnO_3$**. By comparing ceramics with the same grain size but different domain sizes, we observed a significant variation in thermal conductivity, confirming the impact of domains (FIGURE 1). Furthermore, by studying ceramics with both different grain sizes and domain sizes, **the lowest thermal conductivity is observed for the biggest grain size**, which confirms that controlling the domain size is a powerful way to tune the thermal conductivity in this system.

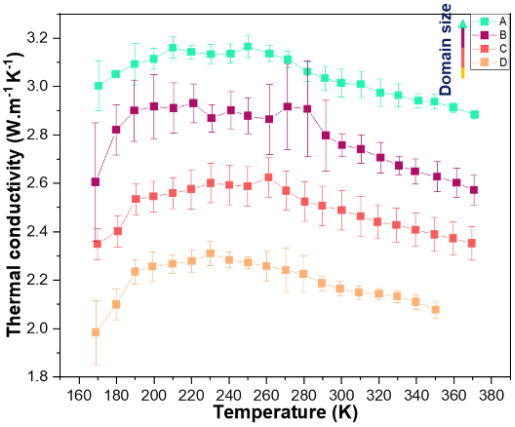

FIGURE 1. THERMAL CONDUCTIVITY FROM 170 K TO 380 K FOR FOUR CERAMICS OF $ERMNO_3$ WITH DIFFERENT DOMAIN SIZES (BUT THE SAME GRAIN SIZE).

ACKNOWLEDGMENT

Funded by the European Union (ERC, DYNAMHEAT, N°101077402). Views and opinions expressed are however those of the authors only and do not necessarily reflect those of the European Union or the European Research Council. Neither the European Union nor the granting authority can be held responsible for them

REFERENCES

[1] Aryana et al. Nat Commun. 13, 1573 (2022).
[2] Limelette et al. Phys. Rev. B. 108, 144104 (2023).
[3] G.F. Nataf et al. Nature Reviews Physics 2, 634 (2020).
[4] J. Schultheiß et al. Adv. Mater. 34, 2203449 (2022).